# Effects of uniaxial strain in hypertrophic cardiomyopathy -patient specific human induced pluripotent stem cell -derived cardiomyocytes

Risto-Pekka Pölönen
University of Tampere
BioMediTech
Heart Group

**PRO GRADU –TUTKIELMA**

Paikka: TAMPEREEN YLIOPISTO
BioMediTech (BMT)
Tekijä: PÖLÖNEN, RISTO-PEKKA JUHANI
Otsikko: Yhdensuuntaisen mekaanisen venytyksen vaikutukset hypertrofista kardiomyopatiaa sairastavista potilaista tuotettuihin indusoiduista pluripotenteista kantasoluista erilaistettuihin sydänlihassoluihin
Sivumäärä: 68
Ohjaajat: Katriina Aalto-Setälä, Marisa Ojala
Tarkastajat: Professori, MD Katriina Aalto-Setälä ja professori Riitta Seppänen
Päiväys: Huhtikuu 2014

---

**Tutkimuksen tausta ja tavoitteet:** Hypertrofinen kardiomyopatia (HCM) on autosomaali-dominantisti periytyvä sairaus joka on sekä geno- että fenotyypiltään hyvin heterogeeninen. HCM on yksi yleisimmistä periytyvistä sydänsairauksista sekä erittäin merkittävä tekijä sydämen komplikaatioista johtuvissa äkkikuolemissa nuorilla aikuisilla. Taudille tyypillinen vasemman kammion- ja kammioiden välisen seinämän sydänlihaksen paksuuntuminen voi johtaa useisiin erimuotoisiin sydämen toiminnallisiin komplikaatioihin. Hoitoa HCM:aa vastaan ei ole vielä löydetty. Tämän tutkimuksen tavoitteena oli identifioida ja verrata yhdensuuntaisen mekaanisen venytyksen vaikutuksia HCM –potilaiden ja kontrollihenkilöiden ihmisen indusoiduista pluripotenteista kantasoluista erilaistettuihin sydänlihassoluihin.

**Tutkimusmenetelmät:** Tutkimuksessa käytettiin neljää eri ihmisen fibroblasteista uudelleenohjelmoitua indusoitua pluripotenttia kantasolulinjaa (hiPSC) joista kolme oli HCM-potilasspesifisiä kantaen suomalaista *MYBPC3*-valtamutaatiota (Q1061X) ja yksi kontrollilinja terveestä henkilöstä. Näistä linjoista erilaistettuja sydänlihassoluja venytettiin yhdensuuntaisesti Flexcell®-laitteella, immunovärjättiin, kuvattiin ja analysoitiin. Immunovärjätyistä kuvista analysoitiin hiPS-soluista erilaistettujen sydänlihassolujen jakautumista, järjestäytymistä, monitumaisuutta, pinta-alaa, sarkomeeriproteiinien organisoitumista sekä kammio- ja eteisspesifisten sydänlihassolujen muodostumista.

**Tutkimustulokset:** Venytettyjä ja venyttämättömiä iPS-soluista erilaistettuja sydänlihassoluja verrattiin keskenään. Venytys vähensi jakaantumista ja monitumaisuutta. Venytys indusoi pinta-alan kasvua villityypin soluissa, eteisspesifisten sydänlihassolujen muodostumista sekä järjestäytymistä venytyksen suuntaa vasten. Venytyksellä oli erilaisia vaikutuksia eri sarkomeeriproteiinien järjestäytymiseen. Verrattaessa HCM- ja kontrolli-sydänlihassoluja keskenään, jakautuminen ja järjestäytyminen olivat samaa luokkaa, monitumaisia sekä eteisspesifisiä HCM -sydänlihassoluja oli enemmän ja kontrollisolut olivat pienempiä pinta-alaltaan.

**Johtopäätökset:** Yhdensuuntaisella mekaanisella venytyksellä on useita eri vaikutuksia hiPS-soluista erilaistettuihin sydänlihassoluihin. Mekaanisesti stimuloimalla hiPSC sydänlihassoluja voidaan saada kypsymään ja paremmin vastaamaan aikuisen kudoksen kypsiä sydänlihassoluja.

**MASTER'S THESIS**


| | |
|---|---|
| Place: | UNIVERSITY OF TAMPERE<br>BioMediTech (BMT) |
| Author: | PÖLÖNEN, RISTO-PEKKA JUHANI |
| Title: | Effects of uniaxial strain in hypertrophic cardiomyopathy -patient specific human induced pluripotent stem cell -derived cardiomyocytes |
| Pages: | 68 |
| Supervisors: | Katriina Aalto-Setälä, Marisa Ojala |
| Reviewers: | Professor, MD Katriina Aalto-Setälä and professor Riitta Seppänen |
| Date: | April 2014 |



**Background and aims:** Hypertrophic cardiomyopathy (HCM) is genetically inherited autosomal-dominant disease with significant genotypic and phenotypic heterogeneity. HCM is one of the most common inherited cardiovascular disorders and the leading cause of sudden cardiac death (SCD) in young adults. Typically hypertrophy affects the left ventricle and interventricular septum and may eventually lead to various cardiac complications. No specific preventive therapy is available for HCM. The aim of this study was to identify and compare the effects of uniaxial mechanical strain on HCM –patient specific and control human induced pluripotent stem cell -derived cardiomyocytes.

**Methods:** Four induced pluripotent stem cell (hiPSC) lines were used in this study. Three cell lines were HCM –patient specific carrying the Q1061X- Finnish founder mutation in *MYBPC3* gene and one wild type cell line was generated from a healthy individual. Cardiomyocytes (CMs) were differentiated from the hiPSC lines by END-2 method, stretched uniaxially by Flexcell®-apparatus, immunostained, imaged and analyzed. From immunostained images, hiPSC –derived CMs' proliferation, alignment, multinucleation, area and sarcomere protein organization were analyzed.

**Results:** Stretched and control hiPSC –derived CMs were compared. Stretching decreased proliferation and multinuclearism. Stretching induced growth of area in wild type CMs, formation of atrial CMs and alignment against the axis of the strain. Stretching had diverse effects on sarcomere protein organization. When HCM and wild type cells were compared, proliferation and alignment were similar, there were more multinuclear and atrial HCM CMs and wildtype CMs were smaller in area.

**Conclusions:** Uniaxial mechanical stretch has diverse effects on hiPSC –derived CMs. By mechanical stimulation, hiPSC –derived CMs could be made more mature to better resemble native adult CMs.

## Acknowledgements

This study was carried out in Heart Group, University of Tampere, BioMediTech. First of all, I would like to thank the leader of the Heart group, Katriina Aalto-Setälä, and my instructor, Marisa Ojala. Also, I would like to thank other members of the Heart group for advice and support, especially Henna Venäläinen, Markus Haponen and Disheet Shah. For collaboration, I would like to thank Jyrki Rasku, UTA SIS. Big thanks goes to all of my friends and family, who have supported me throughout my studies.

Tampere 28.4.2014

Risto-Pekka Pölönen

# Table of contents

- Abbreviations:
    - Action potential, AP
    - Adenylyl cyclase, AC
    - Alpha-myosin heavy chain, α-MHC
    - Alpha-tropomyosin, αTM
    - Atrial myosin light chain 2, MLC2a
    - Atrial natriuretic factor, ANF
    - Beta-myosin heavy chain, β-MHC
    - Beta-adrenergic receptors, β-AR
    - Big MAPK, BMK or ERK5
    - C-Jun N-terminal kinase, JNK
    - $Ca^{2+}$/calmodulin-dependent kinase II, CaMKII
    - Cardiac troponin C, cTnC
    - Cardiac troponin I, cTnI
    - Cardiac troponin T, cTnT
    - Cardiomyocyte, CM
    - Cyclic adenosinemonophosphate, cAMP
    - Dilated cardiomyopathy, DCM
    - Electrocardiography, ECG
    - Excitation-contraction coupling, ECC
    - Extracellular signal-regulated kinase, ERK
    - G-protein coupled receptor, GPCR
    - GPCR receptor kinase, GRK
    - Histone deacetylase, HDAC
    - Human induced pluripotent stem cell, hiPSC
    - Hypertrophic cardiomyopathy, HCM
    - Magnetic resonance imaging MRI
    - Mitogen-activated protein kinase, MAPK
    - Mitogen-activated protein kinase kinase, MAPKK
    - Mitogen-activated protein kinase kinase kinase, MAPKKK
    - Myosin binding protein C, MyBP-C
    - Myosin essential light chain, ELC
    - Myosin regulatory light chain, RLC
    - Protein kinase A, PKA
    - Protein kinase Cα, PKCα
    - Ryanodine receptor, RyR
    - Reactive oxygen species, ROS
    - Restrictive cardiomyopathy, RCM
    - Sarcoplasmic reticulum, SR
    - Sudden cardiac death, SCD
    - Stretch activated channel, SAC
    - Ventricular myosin light chain 2, MLC2v
    - Wild type, WT

# 1. Introduction

Hypertrophic cardiomyopathy (HCM) is genetically inherited autosomal-dominant disease with significant genotypic and phenotypic heterogeneity. HCM is one of the most common inherited cardiovascular disorders and the leading cause of sudden cardiac death (SCD) in young adults. Typically hypertrophy affects the left ventricle and interventricular septum and may eventually lead to various cardiac complications. No specific preventive therapy is available for HCM. (Ashrafian et al., 2003; Maron & Maron, 2013; Watkins et al., 2011.)

Several genes coding for sarcomeric proteins have been associated with HCM (Landstrom & Ackerman, 2010; Maron & Maron, 2013; Watkins et al., 2011). In Finland two founder mutations have been discovered (Jääskeläinen et al., 2013). These mutations are located in genes coding for α-tropomyosin (αTM, *TPM1*) and myosin binding protein C (MyBP-C, *MYBPC3*). HCM is thought to arise from myocardial dysfunction caused by defects in sarcomere proteins and/or aberrant cardiac remodeling (Ashrafian et al., 2003; Maron & Maron, 2013; Watkins et al., 2011). The exact mechanisms are unknown.

In 2006 Takahashi and Yamanaka published a new way to create pluripotent stem cells by inducing mouse embryonic or adult fibroblasts using retroviral vector carrying transcription factors (Takahashi & Yamanaka, 2006). After their significant discovery, the same has been achieved with human somatic cells by several research groups all over the world (Kujala et al., 2012; Lan et al., 2013; Liang et al., 2013; Sun et al., 2012). Human induced pluripotent stem cells (hiPSCs) can be differentiated into any cell type of the human body, including cardiomyocytes (CMs) (Mummery et al., 2012). hiPSCs offer a great platform for cardiac disease modeling and -drug screening, since there are no many human sources of cardiac tissue specimens available. However, hiPSC derived CMs are structurally and functionally immature (Keung et al., 2014; Robertson et al., 2013).

In this study, effects of uniaxial mechanical strain on HCM –patient specific and wild type (WT) hiPSC –derived CMs were studied. Four different hiPSC lines were exposed to uniaxial mechanical strain to analyze its effect on CMs' proliferation, sarcomere proteins, alignment, multinucleation, atrial and ventricular cell formation and area. The HCM cell lines were carrying the *MYBPC3* Finnish founder mutation.

# 2. Literature review

## 2.1 Introduction to heart muscle

The main function of the heart is to pump oxidized blood to peripheral circulation and deoxidized blood to the pulmonary circulation. Heart muscle, i.e. the myocardium, provides the contractile force to cause movement of the blood in the blood vessels by increasing pressure. To carry out this task, myocardium needs to act as a synchronized unit. CMs are the basic unit of the myocardium and they are linked to each other at intercalated discs via cell to cell connections known as connexins, which allow the action potential (AP) to travel from one cell to another (Bers 2001; Severs, 2000). This allows the functional syncytium of the myocardium. There are different kind of CMs in the myocardium: atrial and ventricular CMs, pacemaker cells and purkinje fiber cells. Even though they have many similarities, there are a few know differences. They have different AP rates, myofibrillar contractile forces depending on their purpose and also differences in protein expressions, for example different connexin isoforms. Pacemaker cells are located at the sinoatrial node and are responsible for the pacemaking of the heart. Purkinje fiber cells act as the conduction system for the AP. Ventricular CMs provide the most contractile force whereas pacemaker cells maintain the rhythm of the heart with weak contractile force. (Bootman et al., 2006; Dehaan & Eichna, 1961; Moorman & Christoffels, 2003; Severs, 2000.) In comparison with ventricular CMs, atrial CMs do not have transverse tubules (T-tubules) which means they have different calcium handling properties (Ayettey & Navaratnam, 1978; Yamasaki et al., 1997).

### 2.1.1. Excitation contraction coupling

The pacemaker cells in sinoatrial node are responsible for maintaining the rhythm of the heart. They have the ability to contract without stimulation. The AP generated by them spreads along the conduction system to reach the myocardium. Every CM receives the AP because of the gap junctions. When AP reaches CMs cell membrane, it depolarizes and voltage-dependent calcium channel ($I_{Ca}$) opens letting $Ca^{2+}$ -ions in to the cell. There are two types of $I_{Ca}$: L-type ($I_{Ca,L}$) and T-type ($I_{Ca,T}$) (Bers 2000; Bers 2001; Bers, 2008). $I_{Ca,T}$ is activated at more negative membrane potential than

$I_{Ca,L}$, basically meaning it will be activated more easily. On the other hand, it inactivates more rapidly than $I_{Ca,L}$. These attributes allow more rapid cycle of contraction, of course with other factors, so it does not come as a surprise that $I_{Ca,T}$ is mostly expressed in pacemaker and purkinje cells (Bers 2000; Bers 2001; Bers, 2008).

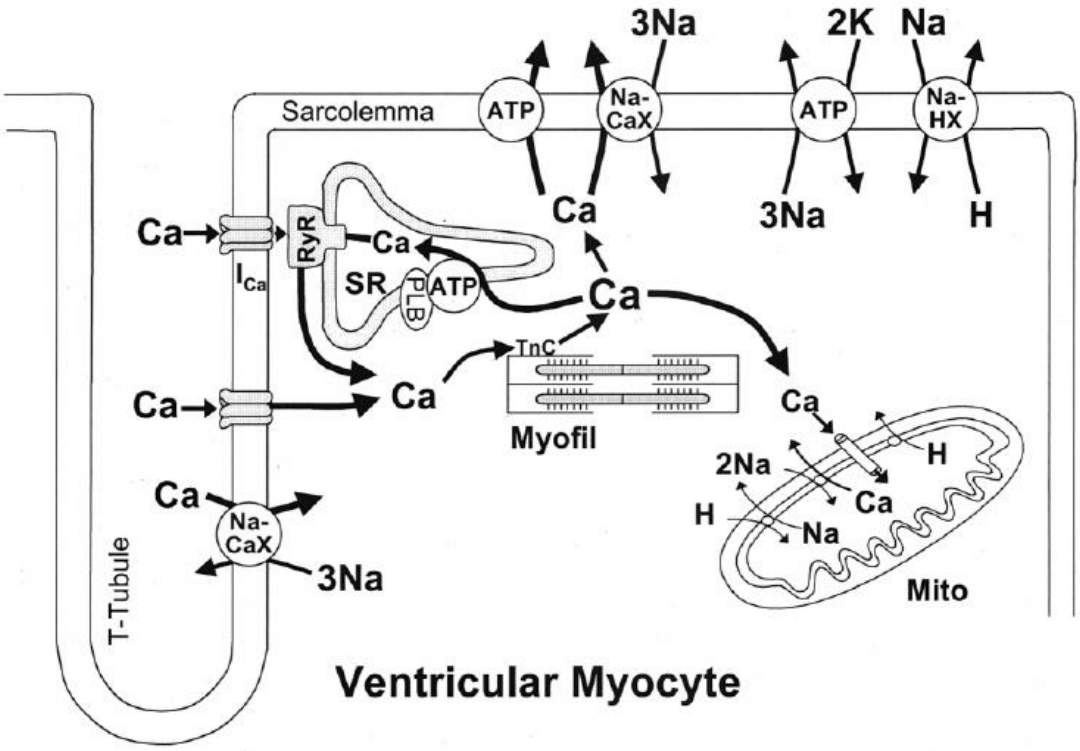


**Figure 1.** Calcium transport in the excitation contraction coupling (ECC) in ventricular cardiomyocytes (Bers, 2000). Calcium transport at peripheral myocyte cell membrane (sarcolemma) includes Ca ATPase (ATP), Na/Ca exchanger (Na-CaX) and at T-tubular sarcolemma voltage dependent calcium channels ($I_{Ca}$) and Na-CaX. Ryanodine receptor (RyR) is at dyadic junctional position on sarcoplasmic reticulum (SR). RyRs contribute to the release of calcium from SR and SR Ca ATPase (SR ATP) to uptake of calcium from cytoplasm. The activity of SR Ca ATPase is regulated by phospholamban (PLB). Cytoplasmic free calcium binds to troponin C (TnC) on the thin filaments and allows the myofibrillar contraction. Calcium enters mitochondria via uniporter and is removed by Na-CaX. Intramitochondrial calcium activates ATP production. Na-K ATPase and Na/H exchanger (NaHX) contribute to the ion balance and potential of the cell.

Activation of $I_{Ca}$ results in increased intracellular [Ca2+] which activates ryanodine receptors (RyRs). This results in the $Ca^{2+}$ -flux out from the sarcoplasmic reticulum (SR), which acts as an internal $Ca^{2+}$ storage of the cell (Bers 2000; Bers 2001; Bers, 2008). This phenomenon is known as calcium-induced calcium-release. In ventricular myocytes, RyRs are mostly located at the SR membrane in the proximity of the T-tubules as junctional RyRs, whereas in atrial myocytes there are larger bulk

of non-junctional RyRs deeper in the cells because of the absence of T-tubules (Bootman et al., 2006; Chen-Izu et al., 2006). This creates slight differences in excitation-contraction coupling (ECC) between atrial and ventricular myocytes, such as positioning of $I_{Ca,L}$ channels. Usually RyRs are located underneath the $I_{Ca,L}$ channels creating dyadic junctions (Figure 1). Because of the lack of T-tubules, these dyadic junctions are present only at the cell membrane (sarcolemma) of the atrial myocytes, whereas in ventricular myocytes they are scattered throughout the T-tubule network. (Bootman et al., 2006; Chen-Izu et al., 2006.) For this reason, influx of calcium creates an uneven balance of intracellular [$Ca^{2+}$] throughout the atrial myocytes after depolarization (Bootman et al., 2006).

There is also some calcium entry to the cells via Na/Ca exchanger antiporter membrane proteins, but the voltage dependent calcium channels carry out most of the task. Free calcium-ions inside the cell bind to troponin C (TnC), one of the three troponins creating the troponin-complex, resulting in a conformational change which allows myosin heads of the thick filament to bind to actins of the thin filament. This conformational change moves long tropomyosin filaments away from the blocking position of actins, resulting in increased myosin binding along the thin filament, called cooperative activation. (Bers 2000; Bers 2001; Bers, 2008.)

Sympathetic and parasympathetic nervous systems regulate the function of the heart muscle by neuroendocrine transmitters, hormones. β-adrenergic receptors (β-AR) bind catecholamines (hormones) such as epinephrine (adrenaline) and norepinephrine (noradrenaline) which activate several downstream signaling pathways in CMs. The hormonal regulation results in altered inotropy, chronotropy and lusitropy (cardiac output, heart rate and relaxation of myocardium) of the CMs by altering the calcium handling inside the cell. (Brodde & Michel, 1999.)

For relaxation to occur, calcium must be exported from the cytoplasm outside of the cell and/or back to SR, to lower the [$Ca^{2+}$] in the cytoplasm so that the calcium-ions can dissociate from TnC and undo the conformational change to block the actins of thin filament again. Calcium can be transported out of the cell by Ca ATPase and Na/Ca exchanger, into SR by SR Ca ATPase and into mitochondria by Ca uniporter. SR Ca ATPase and, to a lesser extent, Na/Ca exchanger constitute the main two elements of lowering the cytoplasmic [$Ca^{2+}$]. (Bers 2000; Bers 2001; Bers, 2008.)

Actomyosin ATPase and active transportation of ions are the two most major consumers of ATP in CMs (Bers, 2008). Mitochondria are the powerhouses of the

cell, so they must adapt to altering energy demands in CMs for example during excercise. Approximately 30% of CM volume is occupied by mitochondria (Bers, 2000). Calcium can enter mitochondria via calcium uniporter, and indeed, intramitochondrial calcium concentration can activate ATP synthase and several dehydrogenases to increase ATP production. Calcium is removed from mitochondria by Na/Ca exchange. (Bers, 2008.)

### 2.1.2. Sarcomere structure

CMs are full of myofibrils which consist of consecutive sarcomeres, the contractive units which are separated by Z-discs (Figure 2) (Clark et al., 2002). Z-discs create a backbone for thin filaments and they consist of myofilament cross-linking proteins such as α-actinin (Chiu et al., 2010; Clark et al., 2002)). The thin filaments consist of actins and αTMs covering them along the filament (Bers, 2001; Clark et al., 2002). αTM is a long helical protein which covers seven actin proteins and overlaps slightly with another tropomyosin following it (Bers, 2001; Tardiff, 2011).

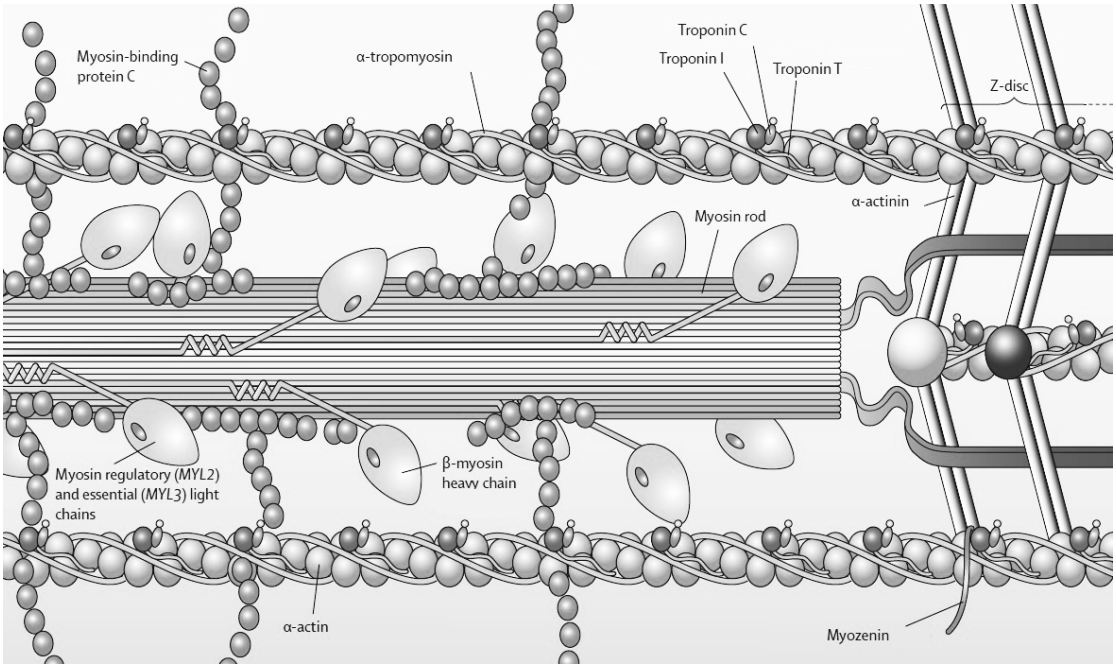


**Figure 2.** Microscopic anatomy of the cardiac muscle showing the sarcomere and the sarcomeric proteins. The complex interaction of proteins driving the events taking place for the contraction and relaxation of the cardiac muscle shown. (Edited from Maron & Maron, 2013)

Along the thin filament, there are troponin complexes which are in close interactions with both actin and αTM. Troponin complex consists of three troponins: troponin I (TnI), troponin C (TnC) and troponin T (TnT) (Metzger & Westfall, 2004; Tardiff, 2011). Thick filament consists of myosin rod from which myosin heads reach towards thin filament (Harris et al., 2011). Sliding of the thin and thick filaments along each other shortens the sarcomere bringing the two Z-discs closer to each other. The myofilaments itself do not shorten in length. The myosin heads are responsible for the interaction between the thick and thin filament and provide the contractile force. The myosin head consists of myosin heavy-, regulatory light- and essential light chains (MHC, RLC and ELC respectively) (Warrick & Spudich, 1987). MyBP-C acts as a cross-bridge between thick and thin filament proteins and it is thought to have regulative and structural properties in the sarcomere (Barefield et al., 2014).

## 2.2. Hypertrophic cardiomyopathy

HCM is a prevalent hereditary cardiac disease which prevalence is thought to be as high as 1:500 (Maron et al., 1995). Although, this is just an approximation and the number can be even greater, since all affected people carrying this genetically inherited disease are not diagnosed. The disease has been studied for over 50 years now, and the various genetic effectors discovered show that it is very heterogenous, both genetically and clinically. There are over 1400 genetic mutations discovered which cause HCM (Maron & Maron, 2013). These mutations are found in 11 or more genes most coding for sarcomeric proteins (Landstrom & Ackerman, 2010; Maron & Maron, 2013). Worldwide, most of the mutations are located in genes coding beta-myosin heavy chain (β-MHC, *MYH7*) and MyBP-C (*MYBPC3*) (Maron & Maron, 2013; Richard et al., 2003; Watkins et al 2011). In Finland, two founder mutations for HCM were recently discovered (Jääskeläinen et al., 2013). These mutations are located in genes coding for αTM (*TPM1*) and MyBP-C (*MYBPC3*).

### 2.2.1. Pathology and signaling in HCM

HCM is often linked to arrhythmia and SCD, especially in young competing athletes (Maron et al., 1980; Maron et al., 1986). In HCM, the heart muscle (myocardium) becomes enlarged because of the thickening of left ventricular and/or interventricular

septal myocardium characterized with myocyte disarray and fibrosis (Figure 3) (Maron & Maron, 2013; Watkins et al., 2011). In some cases there is also right ventricular thickening (Watkins et al 2011). The left ventricle wall thickness can vary a lot, from mild (13-15mm) to massive (>50mm) (Klues et al., 1995; Maron et al., 2009). The methods used to diagnose HCM include electrocardiography (ECG), echocardiography and magnetic resonance imaging (MRI) of the heart (Maron & Maron, 2013). For the last ten years, the most effective treatment for HCM and prevention of SCD has been implantable defibrillators, whereas pharmacological treatment includes beta-blockers, verapamil and disopyramide (Maron & Maron, 2013). However, specific treatment for HCM has not yet been discovered.

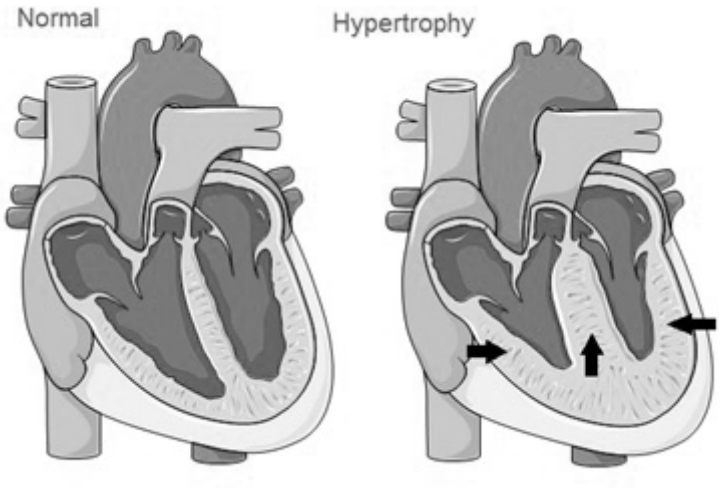


**Figure 3.** Normal and hypertrophied heart. Atrial and left ventricular wall and interventricular septum wall (arrows) thickness increases in cardiac hypertrophy. (Edited from www.servier.com/powerpoint-image-bank)

The exact mechanism how the cardiac hypertrophy develops, is not perfectly clear. However, it is thought to be a combination of changes in calcium affinity of the thin filaments and CM energy consumption (Crilley et al., 2003; Robinson et al., 2007). Mutations in genes coding sarcomeric proteins are thought to have a myofilament activating effect by increasing the calcium affinity on the thin filament, which then leads to hypercontractility and a greater energy consumption of the CM (Crilley et al., 2003; Robinson et al., 2007). Since calcium plays a key role in ECC in CMs, it is no surprise that the alterations in calcium kinetics cause aberrant energy consumption and metabolism. These events are thought to lead to the activation of signaling pathways which cause CMs to grow in size and cause hypertrophy (Lan et

al., 2013). On the other hand, there has been some evidence that some sarcomeric protein mutations could decrease the contractile force of the cardiac myofilaments (Lankford et al., 1995; Watkins et al., 1996). This kind of behavior could lead to a compensatory hypertrophy by forcing the CMs to accommodate to the lack of contractile force (Ashrafian et al., 2003).

Several signaling pathways related to hypertrophy have been studied (Figure 4). β-ARs are a type of g-protein coupled receptors (GPCRs) responsible for many downstream events in cardiac signaling pathways. They activate adenylyl cyclase (AC) and increase intracellular cyclic adenosine monophosphate (cAMP) concentration which leads to increased CM inotropy, chronotropy and lusitropy by activating protein kinase A (PKA) (Brodde & Michel, 1999; Lohse et al., 2003; van Berlo et al., 2013). PKA phosphorylates key calcium handling proteins which then leads to aforementioned phenomena in CMs. This pathway may lose its effect if it is excessively activated during a long period of time, which then may partly affect the development of hypertrophy in cardiac muscle (van Berlo et al., 2013). Another effect of chronic β-AR stimulation is desensitization of the receptor which has negative effects on myocardium. GPCR receptor kinases (GRKs) phosphorylate β-ARs to which β-arrestins then bind, uncoupling the receptor from the G-proteins causing decreased receptor sensitivity (Gurevich & Gurevich, 2006; Lohse et al., 2003). Activation of protein kinase Cα (PKCα), which is induced by GPCRs, regulates intracellular calcium handling proteins and thus myofilament contraction (van Berlo et al., 2013). Even though PKCα does not directly cause cardiac hypertrophy, its expression is elevated in failing human hearts, hence its inhibition could provide a novel therapeutic strategy (Bowling et al., 1999; Dorn & Force, 2005; Hambleton et al., 2007). Intracellular calcium, calmodulin and reactive oxygen species (ROS) regulate the $Ca^{2+}$/calmodulin-dependent kinase II (CaMKII), which acts, in addition to the same type of regulation as PKCα, as a gene transcription regulator by influencing histone deacetylases (HDACs) (Anderson et al., 2011; Erickson et al., 2008; Zhang et al., 2007). Also, the $\delta_B$-isoform of CaMKII, which localizes in nucleus, is shown to induce atrial natriuretic factor (ANF) expression, which is considered as a marker for ventricular hypertrophy (Ramirez et al., 1997). HDACs are key regulators of epigenetics. They deacetylate lysine residues in histone tails which usually leads to a gene repression (Bush & McKinsey, 2010). However, this is not always the case, since there is some evidence about HDAC regulation leading to a gene activation

suggesting that deacetylation/acetylation ratio is fine tuning the expression levels (Wang et al., 2009). HDACs have been identified as regulators of cardiac growth and they have antihypertrophic effects, which could be used in novel therapeutic strategies (Bush & McKinsey, 2010). Mitogen-activated protein kinase (MAPK) pathway, even though well studied, is very complex and its effects are still quite poorly understood. It constitutes several subfamilies including extracellular signal-regulated kinases (ERKs), c-Jun N-terminal kinases (JNKs), p38 kinases, and big MAPK (BMK or ERK5) (Rose et al., 2010). The activation of MAPK leads to activation of a cascade of phosphorylations, where MAPK kinase kinase (MAPKKK) activates MAPK kinase (MAPKK) which in turn activates MAPK (Rose et al., 2010). This activation cascade responses to different stimuli and results in various outcomes, not to mention the complex regulatory system. Even though there are evidence that MAPK pathway induces hypertrophy in heart, the results are somewhat controversial, largely due to the complexity of the pathway and the great number of involved mediators in it (Rose et al., 2010).

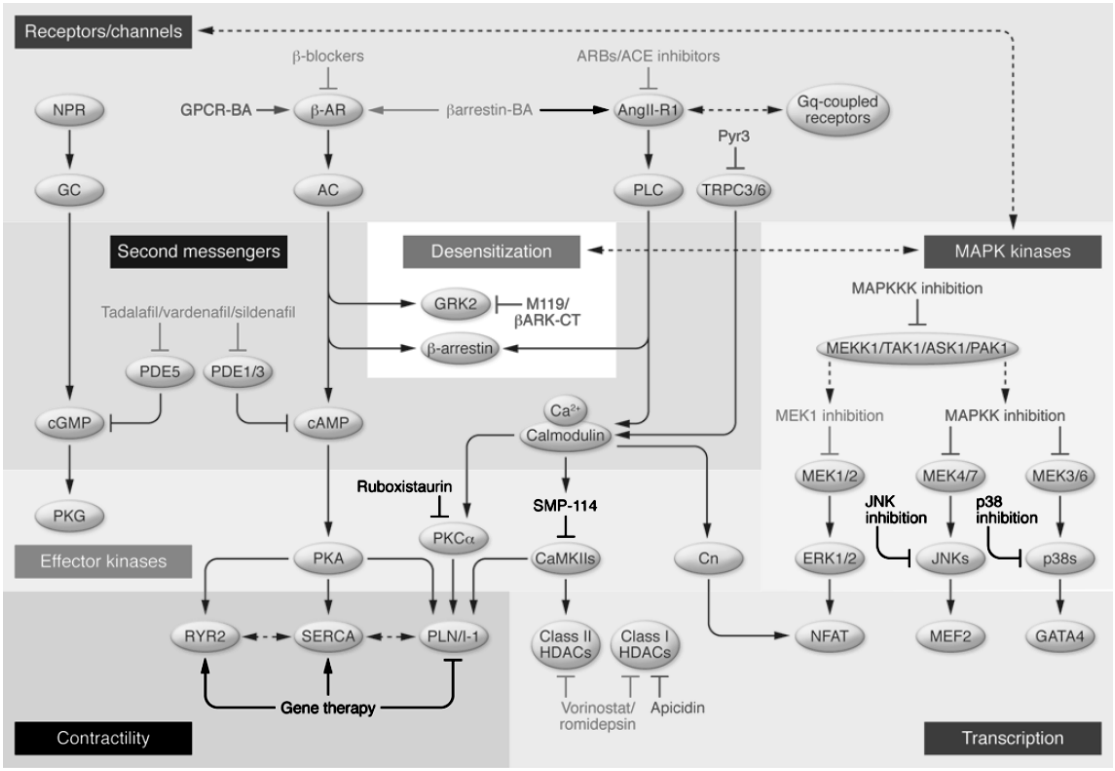


**Figure 4.** Signaling pathways underlying pathologic cardiac remodeling. (Edited from van Berlo et al., 2013)

### 2.2.2. From genotypes to phenotypes

HCM is inherited through autosomal dominant pattern with incomplete age-related penetrance (Landstrom & Ackerman, 2010; Maron & Maron, 2013; Watkins et al., 2011). Over 1400 mutations are found in over 11 genes, most coding for sarcomeric proteins, on top of which may be unique in each family (Landstrom & Ackerman, 2010; Maron & Maron, 2013; Watkins et al., 2011). Every new HCM family member has 50% chance of getting the mutation. These numbers itself tell about the genetic heterogeneity of the disease. Worldwide, most of the mutations are found in genes coding for β-MHC (*MYH7*) and MyBP-C (*MYBPC3*), proportions being 25-35% each of all cases (Maron & Maron, 2013; Watkins et al., 2011). Mutations in the rest of the genes account only for 1-5% of the cases each (Maron & Maron, 2013; Watkins et al., 2011). In Finland the two most common mutations are *TPM1*-D175N and *MYBPC3*-Q1061X accounting for 6.5% and 11.4% of the HCM cases respectively (Jääskeläinen et al., 2013).

**Table 1.** Genes associated with HCM and aberrant cardiac remodeling. (*) Finnish founder mutations. Their respective prevalences in Finland are 11.4 and 6.5%. (Bos and Ackerman, 2009; Jääskeläinen et al., 2013; Landstrom & Ackerman, 2010; Richard et al., 2003; Seidman & Seidman, 2011)

| Gene | Protein | Prevalence in HCM |
|---|---|---|
| Thick filament | | |
| *MYH7* | β-MHC | 25-35% |
| *MYL2* | Regulator myosin light chain | 1-5% |
| *MYL3* | Essential myosin light chain | 1-5% |
| *MYBPC3* | Myosin binding protein C | 25-35%* |
| *MYH6* | α-myosin heavy chain | 1-5% |
| *TTN* | Titin | 1-5% |
| Thin Filament | | |
| *TPM1* | α-tropomyosin | 1-5%* |
| *TNNT2* | Cardiac troponin T | 1-5% |
| *TNNI3* | Cardiac troponin I | 1-5% |
| *TNNC1* | Cardiac troponin C | 1-5% |
| *ACTC* | α-actin | 1-5% |

Genes coding for sarcomeric proteins, which have been shown to cause HCM, are shown in Table 1. Other susceptible genes, such as ACTN2 coding for α-actinin, have also been found (Bos and Ackerman, 2009; Seidman & Seidman, 2011). The top five genes most prone to mutations, according to CG relative mutability, were shown to be *TNNC1, TNNT2, MYH7, MYBPC3* and *MYL2* suggesting that deamination of CpGs could be an important mechanism for mutation development (Meurs & Mealey, 2008). *MYH7* and *MYBPC3* mutations account 60-70% of the HCM cases, which suggests a highlighted role of thick filament in development of HCM (Maron & Maron, 2013; Morita et al., 2006).

Mutations in *MYBPC3* have been shown to cause familial HCM in elderly indicating a late onset of the disease whereas mutations in *MYH7* and *TNNT2* cause symptomatic HCM early in life (Niimura et al., 2002). There are numerous missense and nonsense mutations, deletions and insertions and splice site donor/acceptor mutations reported in *MYBPC3* leading to a premature STOP-codon, reading frame shifts or even truncated protein (Harris et al., 2011). Despite mouse models showing truncated proteins lacking C-terminal myosin and titin binding sites, showing increased calcium sensitivity of tension and inadequate localization in sarcomeres, results from human biopsies have been in contradict, showing reduced amounts of MyBP-C, thus indicating its degradation caused by post-translational modification of misfold protein (Marston et al., 2009; van Dijk et al., 2009; Yang et al., 1999). This has led to a hypothesis that *MYBPC3* truncation mutations cause HCM through haploinsufficiency. However, reduced MyBP-C amounts were also reported with a mutation in *MYBPC3* leading to a single amino acid substitution (Marston et al., 2009). Missense mutations leading to single amino acid substitutions cause more benign outcomes of HCM (Harris et al., 2011). MyBP-C includes domains C0-C10 plus proline/alanine-rich linker sequence between C0 and C1 and a regulatory linker motif between C1 and C2 (Figure 5). The mutations occur throughout the *MYBPC3* gene except the linker sequence appears to somehow have tolerance to mutations, whereas there are a few mutation rich areas in the C3 sequence (Harris et al., 2011). Some of these mutations leading to single amino acid substitutions are thought to lead to MyBP-C malfunction or misfolding, whereas some mutations do not seem to affect the protein folding (Harris et al., 2011). Even though MyBP-C has been studied for almost 40 years, its functional domains' relevancy in thick and thin filament interactions still remains controversial (Bhuiyan et al., 2012). Mutations in these

domains involving protein-protein interactions may have detrimental effects in MyBP-C and sarcomere function, leading to HCM.


**Figure 5.** Domains of MyBP-C. PA = proline/alaninen-rich linker sequence, M = phosphorylable regulatory linker motif. C1, C2 and C7-C10 are involved in protein-protein interactions. Domain C3 has a few mutation "hot spots". Domains C0-C10 all have tertiary structures whereas PA and M are linker domains. C6, C7 and C9 have fibronectin-like and the rest C-domains have immunoglobulin-like folds.

Mutations in *MYH7*, a gene coding for β-MHC, were the first to be found as a causing factors for HCM by Jarcho et al. (1989) and Geisterfer-Lowrance et al. (1990). Eventually, more were found and they were found to account most of the HCM cases (Watkins et al., 1992; Woo et al., 2003). Most of them are related to four important structural and functional domains in the myosin head: actin binding site, ATP binding site, essential light chain binding interface and head–rod junction (Rayment et al., 1995; Woo et al., 2003). Thus mutations cause different clinical outcomes depending on the site of the mutation in the *MYH7* sequence (Fananapazir & Epstein, 1994; Niimura et al., 2002; Woo et al., 2003). Most of the mutations are missense mutations, some which may lead to a charge change of amino acid and cause structural and functional changes resulting in different clinical outcome and disease prognosis (Woo et al., 2003). The α-myosin heavy chain (α-MHC) is an isoform of β-MHC with distinct functional properties. Mutations in *MYH6* were suggested to result in a different clinical outcome, a late onset of HCM by Niimura et al., (2002).

There are two isoforms of ELC and RLC, atrial and ventricular (Schiaffino & Reggiani, 1996). The ventricular isoform of ELC is linked to HCM. Mutations in *MYL3*, the gene coding ELC, are usually located in exons coding for EF-hand domains, which are part of $Ca^{2+}$-binding domain superfamily (Harris et al., 2011). However, in ELC, these domains have lost their ability somewhere along the evolution to bind these divalent cations. Despite the fact, biopsies from patients with mutation in ELC area coding for the EF-hand domain seem to have altered contractile functions (Poetter et al., 1996). The atrial and ventricular isoforms of RLC are also known as MLC2a and MLC2v respectively. In *MYL2*, the gene coding RLC, there are splice site acceptor- and missense mutations reported linked to HCM (Harris et al.,

2011). These mutations affect mainly two domains: an EF-hand domain which binds $Ca^{2+}$ and $Mg^{2+}$ and a highly conserved N-terminal serine residue which mediates positive inotropic and chronotropic effects when phosphorylated (Colson et al., 2010; Harris et al., 2011). The mutations affect these domains' abilities to perform which alters their aforementioned attributes.

Almost 100 independent mutations in thin filament proteins are found to cause HCM (Tardiff, 2011). Like in thick filament proteins, in thin filament mutations in different locations also result in various different clinical outcomes. From thin filament proteins, αTM, actin, cTnC, cTnI and cTnT have been associated with HCM. Although, some mutations in cTnI and cTnT have been associated with another two types of cardiac hypertrophy: dilated cardiomyopathy (DCM) and restrictive cardiomyopathy (RCM) (Tardiff 2011). cTnT was one of the first thin filament proteins shown to cause HCM when mutated (Lin et al., 1996; Morimoto et al., 1998; Redwood et al., 2000; Watkins et al., 1995). It is a key protein acting as an adapter between the troponin-complex and α-TM and actin. There are two alfa-helical domains in cTnT: the N-terminal αTM binding domain and troponin-complex (cTnI and cTnC) binding domain closer to the C-terminus. Mutations in cTnT causing HCM have been identified to localize to the N-terminal domain resulting in increased $Ca^{2+}$ sensitivity of myofilament activation (Tardiff, 2011). Because of the important role of cTnT in myofilament activation, it may not be a surprise that the mutations in this protein result in severe clinical outcome of SCD, but, however, at the same time to a relatively mild left ventricular hypertrophy (LVH) (Watkins et al., 1995). The latter though may partly explain the relatively low frequency of cTnT mutations linked to HCM, since LVH is a characteristic feature of HCM and therefore patients with mutations in cTnT do not appear in study cohorts as much.

cTnC and cTnI create the essential functional part of the troponin-complex responsible for $Ca^{2+}$ induced myofilament activation. There are three $Ca^{2+}$ binding sites in TnC of which the two locating in the N-terminal lobe of the protein regulate interaction with TnI. In the presence of calcium, TnI binds to TnC rather than actin of thin filament, thus not blocking the myosin actin interaction. Even though the importance of cTnI in troponin-complex, mutations in it are very heterogenous and result in various disease patterns (Mogensen et al., 2004). From the structural point of view, most of the mutations are clustered in the highly charged inhibitory region and αTM binding mobile domain in the *TNNI3* amino acid -sequence (Tardiff, 2011).

These two regions are the ones that interact with either TnC or actin depending on the presence of calcium. Therefore it is no surprise that HCM causing mutations in these regions often lead to increase in $Ca^{2+}$ sensitivity of the acto-myosin ATPase, which transforms the chemical energy of ATP to mechanical work of the sliding filaments (Tardiff, 2011).

αTM consists of two alpha-helical chains arranged as coiled-coil. It stabilizes the actin structures and cooperatively with other αTMs acts as a regulator of the myofilament activation by blocking or revealing the actin for the myosin depending on the $Ca^{2+}$ concentration. Mutations causing HCM in *TPM1* have been found to cluster in two regions which are responsible for actin and troponin-complex interactions (Tardiff, 2011). These mutations are also thought to lead into an increased $Ca^{2+}$ sensitivity of myofilament activation (Tardiff, 2011). Clinical outcome varies greatly among patients having *TPM1* mutations.

There are also other genes associated with HCM causing mutations which do not code for myofilament proteins, such as LIM binding domain 3 (*LBD3*), muscle LIM protein (*CSRP3*), telethonin (*TCAP*), vinculin/metavinculin (*VCL*), myozenin 2 (*MYOZ2*), juctophilin-2 (*JPH2*) and phospholamban (*PLN*) (Bos and Ackerman, 2009). Frequencies of the mutations in these genes are usually very low.

Genetic heterogeneity of HCM rises from two different things. First, the SCD in young adults acts kind of as a natural selection to delete these HCM mutations from populations. Second, larger genes attract more mutations because they are supposed to happen completely randomly in the genome (Seidman & Seidman, 2011). Additionally, the role of founder mutations in geologically and sociologically isolated populations is increased because of the more homogenous gene pool. More interestingly, the founder mutations almost always include *MYBPC3* mutations resulting in expression of truncated protein (Seidman & Seidman, 2011). This indicates that the other HCM mutations may have more serious clinical outcome of the disease than founder mutations.

Phenotypic variability is high in HCM (Maron & Maron, 2013; Seidman & Seidman, 2011; Watkins et al., 2011). Even within the members of the same family phenotype may vary depending on genetic, allelic and epigenetic features, not to mention environmental aspects. Earlier studies reported severe forms of HCM but in the present, with better knowledge and diagnostics of the disease, most of the cases feature only mild or atypical symptoms (Watkins et al., 2011). Penetrance of HCM

increases with age, but the onset is observed by peaks both during childhood and mid-adulthood (Watkins et al., 2011). The left ventricular wall undergoes remodeling during the early phase (age <17 years) of life which after tend to complete upon physical maturation (Maron & Maron, 2013). However, there may be delayed onset of HCM later in the ages of >30 years and beyond, but usually the outcome stays quite modest (Maron & Maron, 2013). The question is why children remain asymptomatic.

### 2.2.3. Finnish founder mutations

Founder mutation causing HCM has been discovered in Netherlands, Japan, South Africa and Finland (Alders et al., 2003; Jääskeläinen et al., 2013; Kubo et al., 2005; Moolman-Smook et al., 1999). These kind of mutations may have great impact on the disease in genetically isolated, less heterogenic populations, such as Finnish. In Finland indeed, there are two founder mutations reported: D175N missense mutation in the gene coding αTM (*TPM1*) and Q1061X nonsense mutation in the gene coding myosin-binding protein C (*MYBPC3*) (Jääskeläinen et al., 1998; Jääskeläinen et al., 2002). Together these two mutations account for almost 18% of all HCM cases in Finland.

The reason for why these two mutations are not found to be common in other studied populations around the world, is thought to be the genetic isolation of Finnish population, which has allowed the enrichment of these two particular mutations in Finnish gene pool (Jääskeläinen et al., 2013). However, regional differences in prevalence between these two mutations are seen inside Finnish borders. Also, the size of the study group allows only rough estimations, but in the future, more screenings are expected to be carried out.

## 2.3. Introduction to mechanotransduction

Cell membrane, nucleus and all organelles are connected by a network of cytoskeletal actin filaments and microtubules. Focal adhesion complexes associated with integrins sense the signals coming from extracellular matrix (ECM), which leads to modifications in cytoskeletal scaffold (Chen, 2008). The local mechanical stimulus at the cell membrane becomes propagated through a series of force-dependent interactions which activates signaling pathways inside the cell through

mechanotransduction (Chen, 2008). It is known that mechanical stimulus is important for tissue growth, development and maintenance. Right kind of mechanical stimulus could be even used to drive cell/tissue differentiation into a desirable direction, since mechanical forces are known also to affect cellular signaling, gene expression and cell function (Chen, 2008).

### 2.3.1. Mechanotransduction in cardiomyocytes

Transduction of physical force to a chemical signal can occur through protein conformational changes. These proteins often have linkages to the intracellular cytoskeleton and/or ECM which amplify the signal to the transducers (Orr, 2006). Stretch activated ion channels (SACs), integrins, ECM and focal adhesion kinases may all contribute to the sensing of mechanical stimuli in CMs (Lammerding et al., 2004). SACs play a major role in stretch activated currents in non-selective cation transportation. It has been shown that cariomyocytes from different species respond to mechanical strain with sarcolemma depolarization, AP prolongation and extra systoles (Kamkin et al., 2000; Kamkin et al., 2003). Integrins are a family of heterodimers consisting of 18 different α- and 8 different β-subunits. They have large extracellular ECM binding- and smaller intracellular cytoskeleton binding domain. The intracellular domain can also bind to signaling molecules such as focal adhesion kinase (FAK) and GTPases Rho and Rac (Lammending et al., 2004). Signaling via integrins work both ways, outside-in and inside-out. They can transmit the signal directly via conformational change or indirectly via parts cytoskeleton (Lammerding et al., 2004). The transmitters of mechanical force in CMs have been also found to include complexes which include vinculin, talin and laminin in addition to integrins (Lammerding et al., 2004).

Cardiomyocytes react with transient and long-term responses to various mechanical stimuli to stabilize their environment (Lammerding et al., 2004). Calcium handling can be an example of a transient and structural remodeling of a long term responses. CMs can harness the energy from changes in mechanical environment and stimuli to convert them into growth signals which then can lead to parallel sarcomere deposition and hypertrophy (Sadoshima and Izumo, 1997). In mice stretch activation/stressing of CMs has been shown to induce hypertrophy via increased protein synthesis, gene activation and several signaling pathway activation

(Sadoshima and Izumo, 1997). Paracrine and autocrine growth factors are supposed to be major contributors in the pathogenesis of stretch induced hypertrophic cell growth. In rat CMs, secretion of angiotensin II, endothelin-1 and basic fibroblast growth factor (FGF) are shown to be induced by mechanical stress (Sadoshima and Izumo, 1997). Comparing the responses of mechanical stretching and angiotensin II induction in neonatal rat CMs, several similarities has been found, such as increases in protein synthesis and immediate early-, fetal- and growth factor -gene activation (Sadoshima and Izumo, 1997). There is also similarities in activation of second messengers of mechanical stretch and angiotensin II induction including several kinases and other molecules (Sadoshima and Izumo, 1997). According to these findings it appears to convey that angiotensin II is the primary mediator of stretch induced hypertrophy, at least in rat CMs.

Also, several other stretch activated signaling pathways have been identified in rat CMs: G-protein coupled-, MAPK, janus-associated kinase/signal transducers and activators of transcription- (JAK/STAT), PKC, phospholipase -, calcineurin- and intracellular calcium pathways (Lammerding et al., 2004; Sadoshima and Izumo, 1997). The relevance of some of these in HCM are explained in previous chapter (2.2.2., Figure 3) MAPKs such as ERKs and JNKs phosphorylate substrates responsible for cell growth and differentiation (Sadoshima and Izumo, 1997). JAKs become phosphorylated upon ligand binding to cytokine receptors which lead to phosphorylation and further activation of STATs, which are transcription factors (Lammerding et al., 2004). GPCRs can also activate STATs which leads to gene activation. The role of calcium in CMs is explained in previous chapter (2.1.1.). Increase in intracellular calcium in CMs increases phospholipase C (PLC) activity, which leads to another downstream events (figure 3). Calcineurin is activated by calcium/calmodulin and it activates JNK and PKC mediating calcium signaling in CMs (Lammerding et al., 2004). As we see, many stretch activated signaling pathways induce HCM, and that furthermore establishes the solid connection between these two events.

## 2.4 Induced pluripotent stem cells

In 2006 Takahashi and Yamanaka published a new way to produce pluripotent stem cells by inducing mouse embryonic or adult fibroblasts using retroviral vector

carrying transcription factors (Takahashi & Yamanaka, 2006). There are four important transcription factors which are required for induction of pluripotency: Oct-3/4, Sox2, c-Myc and KLF4 (Takahashi & Yamanaka, 2006). In 2007, induced pluripotent stem cells (iPSCs) were generated from adult human somatic cells (Takahashi et al., 2007). Human iPSCs (hiPSCs) allow negating the ethical issues arising from the use of human embryonic stem cells (hESCs) in research. Also, they allow easier development of patient- or disease specific cell lines, which offers a great tool for drug screening or to study disease mechanisms. hiPSCs are especially useful to study genetically inherited diseases affecting tissues which are difficult to acces, like heart. Several cardiovascular and neurological diseases have been studied with iPSCs: Long-QT –syndromes, catecholaminergic polymorphic ventricular tachycardias, Alzheimer's and Huntington's diseases for example (Bellin et al., 2012). hiPSCs have the same properties as hESCs: indefinite proliferation and ability to form all types of somatic cells of human body (Bellin et al., 2012). In addition to Yamanaka's original method in which the integrative retroviral vectors were used, there are other methods developed for reprogramming hiPSCs, such as non-integrative vectors, synthetic mRNAs and small molecules (Bellin et al., 2012). The benefits of these are the avoidance of insertional mutagenesis and transgene reactivation, which lowers the risk of tumor formation and cancer risk and also variability between generated cell lines (Bellin et al., 2012). A con of these methods is usually lower efficiency (Bellin et al., 2012).

### 2.4.1. hiPSC -derived CMs

Human iPSCs can be differentiated into any somatic cell of the human body, including CMs. The differentiation of CMs, cardiogenesis and development of early cardiac mesoderm is controlled by three key families of protein growth factors: bone morphogenic proteins (BMPs), wingless/INT proteins (WNTs) and fibroblast growth factors (FGFs) (Mummery et al., 2012). Once these factors have initiated the cardiogenesis by inducing the cardiac mesoderm, complex combination of transcription factors and gene regulatory networks activate and begin a cardiac transcriptional program which leads to proliferation and maturation of CMs (Mummery et al., 2012). The ability to produce CMs *in vitro,* has been a great step forward when considering studies of cardiac diseases. It has been very difficult to

study cardiac diseases without this kind of model before, when one have had to rely on animal models and restricted amount of biopsies and tissue samples. There are three major different ways to differentiate CMs: embryoid body (EB) -method, monolayer culture and inductive co-culture (Mummery et al., 2012). There are usually cell line-to-cell line variation after differentiation, depending on the origin of the cells, reprogramming method and natural variation, resulting in a heterogenous population of rather immature cells (Bellin et al., 2012).

In EB-method, hiPSCs are either partially dissociated and cultured on standard cell culture plates or fully dissociated and cultured on special patterned plates to control EB formation (Mummery et al., 2012). EBs are spontaneous spheroid-like 3D-structures of aggregated pluripotent stem cells with an ability to form all three germ layers (Mummery et al., 2012). EBs develop spontaneously beating CMs. In monolayer culture method, hiPSCs are dissociated and propagated as a simple monolayer- or matrix sandwich culture using Matrigel coated cell culture plates (Mummery et al., 2012). Addition of medium-Matrigel –mix on top of the cell layer creates the sandwich culturing structure (Mummery et al., 2012). With monolayer method, diffusion of nutrition and growth factors is more controlled and reproducible. Inductive co-culture method includes use of visceral endodermal-like END2 –cells which are used for their cell-signaling properties to promote cardiogenesis (Mummery et al., 2003). With this method, it is possible to get spontaneously beating differentiated CMs from relatively small amount of cells. Distinct differentiation-methods require specific growth factors for optimized CM differentiation (Mummery et al., 2012).

# 3. Aims

The aim of this study was to identify and compare the effects of uniaxial mechanical strain on HCM –patient specific and control hiPSC -derived CMs, and learn to use the equipment and methods used in the study, such as cell culturing, Flexcell® –apparatus, immunostaining, imaging and image analyses.

# 4. Materials & methods

## 4.1. Patient-Specific hiPSC lines and culturing

Four cell lines were used in this study: UTA.05105.HCMM, UTA.06108.HCMM, UTA.07108.HCMM and UTA.04602.WT. Three HCM-specific hiPSC lines (UTA.05105.HCMM (46, XX), UTA.06108.HCMM (46, XY) and UTA.07108.HCMM (46, XY)) have been generated from dermal fibroblasts of patients carrying a *MYBPC3*-Q1061X nonsense mutation. Control hiPSC line UTA.04602.WT (46, XX) has been generated from dermal fibroblasts of a healthy 55-year-old female. The collection of biopsies for generating patient specific hiPSC-lines was approved by the ethical committee of Pirkanmaa Hospital District (Aalto-Setälä R08070) and written informed consent was obtained from all the donors. All hiPSC-lines have been established by retroviral transfection of Oct3/4, Sox2, KLF4 and c-Myc (Ohnuki et al., 2009). Characterization of hiPSCs included confirmation of mutations by qPCR, karyotype analysis, confirmation of gene expression by PCR and protein expression by immunocytochemistry. The pluripotency of hiPSC lines was confirmed by EB-formation and teratoma formation in mice.

Human iPSCs were cultured on mitomycin-C inactivated mouse embryonic fibroblasts (MEFs, 26 000 cells/cm$^2$, Merck Millipore, MA, USA), which act as feeder cells to support growth of undifferentiated hiPSCs and to maintain their pluripotent state in hES-medium (Table 2). The undifferentiated state of hiPSCs was confirmed by morphologic analysis and undifferentiated colonies were passaged weekly on new MEFs.

## 4.2. Cardiomyocyte differentiation

Differentiation into CMs was carried out by co-culturing hiPSCs with murine visceral endoderm-like (END-2) cells (prof. Mummery, Humbrecht Institute, Utrecht, The Netherlands) (Mummery et al, 1991). END-2 –cells were mitomycin-C (Sigma Aldrich, MO, USA) inactivated (5µl/ml, 3h), trypsinized (Lonza, Switzerland) and plated on 12-well-plate (Nunc) 175 000 cells/well in END-2 medium (Table 3). END-2 –cells were let to attach in 37°C overnight. 0% KO-SR hES –medium was changed to END-2 cells an hour before plating the hiPSCs. MEFs were removed and undifferentiated hiPSC -colonies were detached by scraping. hiPSC -colonies were

transferred on END-2 –cells ~30 colonies/well with minimal amount of culture medium. Cells were co-cultured in 37°C and 5% $CO_2$. The 0% KO-SR hES -medium was changed at days 5, 8 and 12. At day 14, the medium was changed to 10% KO-SR hES –medium (Table 5) and changed 3 times a week. Cells were monitored with phase-contrast microscopy (Nikon Eclipse TS100 microscope, Imperx IGV-B1620M-KC000 camera, JAI Camera Control Tool software). hiPSC -colonies formed spontaneously beating areas after around 15 days of co-culturing.

**Table 2.** hES-medium (20% KO-SR DMEM). Pen/Strep = 10 U/ml Penicillin + 10 U/ml Streptomycin.

| Component | Quantity |
|---|---|
| Knock-Out DMEM (Life Technologies) | |
| Knock-Out Serum Replacement (KO-SR, Life Technologies) | 20% |
| Non-essential amino acids (NEAA, Fischer Scientific) | 1% |
| GlutaMax (Life Technologies) | 2 mM |
| Pen/Strep (Fischer Scientific) | 50 U/ml |
| 2-mercaptoethanol (Life Technologies) | 0.1 mM |
| Basic fibroblast growth factor (bFGF, R&D Systems) | 4ng/ml |

**Table 3.** END-2 –medium.

| Components | Quantity |
|---|---|
| DMEM-F12 (Life Technologies) | |
| FBS (Immunodiagnostic) | 7.5% |
| NEAA | 1% |
| GlutaMax (Life Technologies) | 2 mM |
| Pen/Strep | 50 U/ml |

**Table 4.** 0% KO-SR hES –medium.

| Components | Quantity |
|---|---|
| KO-DMEM (Life Technologies) | |
| NEAA (Fischer Scientific) | 1% |
| GlutaMax (Life Technologies) | 2 mM |
| Pen/Strep (Fischer Scientific) | 50 U/ml |
| 2-mercaptoethanol (Life Technologies) | 0.1 mM |
| Ascorbic acid ( Sigma Aldrich) | 3.0 mM |

**Table 5.** 10% KO-SR hES –medium.

| Components | Quantity |
|---|---|
| KO-DMEM (Life Technologies) | |
| KO-SR (Life Technologies) | 10% |
| NEAA (Fischer Scientific) | 1% |
| GlutaMax (Life Technologies) | 2 mM |
| Pen/Strep (Fischer Scientific) | 50U/ml |
| 2-mercaptoethanol (Life Technologies) | 0.1 mM |

## 4.3. Dissociation of beating cardiomyocytes

At day 16, spontaneously beating areas of cell colonies were cut and isolated with scalpel, collected in culture medium (10% KO-SR hES -medium) and dissociated (Mummery et al., 2003). Beating areas were washed in Low-Ca buffer (buffer 1, Table 6) at RT for 30 minutes and after that treated with collagenase A (Roche Diagnostics, Switzerland) (buffer 2, Table 6) at 37 ˚C for 45 minutes to one hour. Cells were incubated in KB medium (buffer 3, Table 6) (20µl of 1M glucose was added to 1ml of buffer 3) at RT for one hour. Aggregates/clumps were resuspended in EB-medium (20% FBS in KO-DMEM) (Table 7) by pipetting up and down several times against the bottom of the dish. This is a key step in dissociation, since aggregates, depending on the size, can be hard to break into single cell suspension, but at the same time, cells may be damaged. Single cell suspension was dealt to Uniflex-membranes (3 beating areas/well) and gelatin coated cover slips (1 beating area/well) and let to attach at 37 ˚C for 30-45 minutes before loading up to the final amount of

EB-medium (3ml/well on Uniflex-plates and 800µl/well on 4-well-plates). Cells were cultured for three days before beginning of the stretching experiments.

For immunostaining control samples, 13mm cover slips were washed with 70% ethanol and dried in laminar hood. Coverslips were coated with 0.1% gelatin at RT for one hour.

**Table 6.** Components of dissociation buffers.

| | Low-Ca (1) | Enzyme (2) | KB (3) |
|---|---|---|---|
| NaCl | 12 ml (1M) | 12 ml (1M) | - |
| $CaCl_2$ | - | 3 µl (1M) | - |
| $K_2HPO_4$ | - | - | 3 ml (1M) |
| KCl | 0.54 ml (1M) | 0.54 ml (1M) | 8.5 ml (1M) |
| $Na_2ATP$ | - | - | 2 mmol/L |
| $MgSO_4$ | 0.5 ml (1M) | 0.5 ml (1M) | 0.5 ml (1M) |
| EGTA | - | - | 0.1 ml (1M) |
| Na pyruvate | 0.5 ml (1M) | 0.5 ml (1M) | 0.5 ml (1M) |
| Glucose | 2 ml (1M) | 2 ml (1M) | 2 ml (1M) |
| Creatine | - | - | 5 ml (0,1M) |
| Taurine | 20 ml (0.1M) | 20 ml (0.1M) | 20 ml (0.1M) |
| Collagenase A | - | 1 mg/ml | - |
| HEPES | 1 ml (1M) | 1 ml (1M) | - |
| pH correction | NaOH | NaOH | - |
| pH | 6.9 | 6.9 | 7.2 |

**Table 7.** EB-medium.

| Components | Quantity |
|---|---|
| KO-DMEM (Life Technologies) | |
| FBS (Immunodiagnostic) | 10% |
| NEAA (Fischer Scientific) | 1% |
| GlutaMax (Life Technologies) | 2 mM |
| Pen/Strep (Fischer Scientific) | 50U/ml |

## 4.4. Flexcell®-experiments

Flexcell® is a commercially available device for culturing cells in a mechanically active environment. Flexcell® unit includes controller unit, compressor pump, PC and baseplate with collagen coated Uniflex®-plates with Arctangle® Loading Stations™ (Flexcell®, NC, USA). Pump, controller unit and baseplate are connected with tubes for carrying the negative pressure (suction). There are filters with containers for condensing moisture in the tubing between the baseplate and controller unit. PC and controller unit are connected with Ethernet-cable. The main idea how the uniaxial stretch is created with Flexcell®, is applying suction under the Uniflex-membranes so the membrane will stretch over the edges of loading stations (Figure 6). For creation of non-stretched control samples, loading stations can be left out and STOP-gums made of rubber placed under the Uniflex-membrane to prevent the stretching.

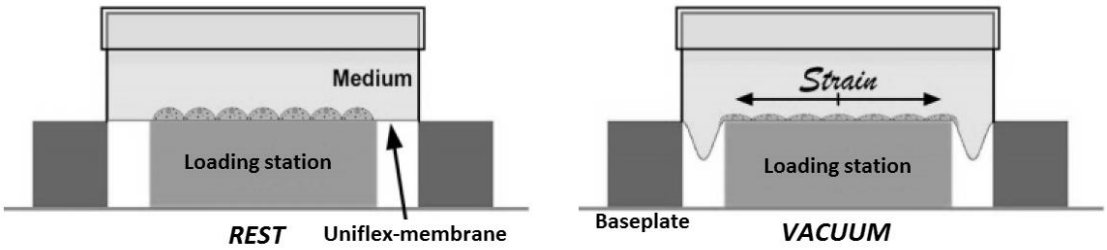


**Figure 6.** Principle of concept: stretching of Uniflex-membranes. At rest, Uniflex-membrane lies steady over the loading station. During stretching, vacuum drags Uniflex-membrane over the edges of loading station creating uniaxial strain. (Edited from Flexcell® Culture Plate & Loading Station User's Manual)

Total of five Flexcell®-experiments were carried out in this study. Because of the novel nature of this study, there were some practical differences between experiments. Regimens, methods and even equipment were changed and modified to make improvements in the study setup. Before use, baseplate and loading stations were washed with 70% EtOH. Loading stations were placed on the baseplate under each Uniflex-plate well. Silicone lubricant was used to minimize the friction between the loading stations and Uniflex-membranes. Additional filter for preventing the moisture reaching the controller unit was installed between experiments 4 and 5. Stretching with cells was carried out in an incubator at 37°C and 5% $CO_2$ while the baseplate with its content was placed in it. At each time point, stretching had to be stopped for the duration of medium change for the remaining Uniflex-plates and sample acquisition. This took usually no more than 30 minutes. At each time point, one

Uniflex- and one 4-well-plate was removed from the stretching-experiment for immunostaining. Removed Uniflex-plate was replaced with an empty Uniflex-plate on the baseplate.

### 4.4.1 The 1st Flexcell®-experiment: UTA.05105.HCMM

The first Flexcell®-experiment was done using UTA.05105.HCMM cells (passage 53) to get to know the Flexcell®-equipment and practice its use. The cells were 20 days of age counted from the start of the END-2 co-culture. Time points for this first stretching were 1, 4, 7 and 9 days. These values were chosen quite randomly based on literature compiled at Flexcell® –website (http://www.flexcellint.com/PDF/FlexcellPublications.pdf). Coverslip-controls were not used in this experiment, because Uniflex-membranes' autofluorescense was not yet observed. Total of 72 beating areas were cut, dissociated and plated on Uniflex-plates. On each Uniflex-plate, three wells were blocked with STOP-gums and used as controls, and three wells were stretched. EB-culture medium was changed 3 times a week. Regimen used for stretching is shown on the Table 8. Proteins studied in this experiment were the following: cardiac troponin-T (cTnT), MyBP-C, α-actinin and connexin-43.

**Table 8.** Regimen used during 1st and 2nd Flexcell® stretching on UTA.05105.HCMM.

| step | wave form | frequency (Hz) | elongation % | time |
|---|---|---|---|---|
| 1 | sin | 0.5 | 2.5 | 3:20 |
| 2 | sin | 0.5 | 5 | 3:20 |
| 3 | sin | 1 | 7.5 | 3:20 |
| 4 | sin | 1 | 10 | 4, 7, 11 and 14d |

### 4.4.2. The 2nd Flexcell®-experiment: UTA.05105.HCMM

The second Flexcell®-experiment was done using UTA.05105.HCMM cells (passage 53, age 20d). The time points were chosen as 4, 7, 11 and 14 days, based on the images of the first Flexcell®-experiment (data not shown). These time points were used in the rest Flexcell®-experiments. Total of 84 beating areas were cut, dissociated and plated on four Uniflex-plates and 8 coverslips on four 4-well-plates. On each

Uniflex-plate, two wells were blocked with STOP-gums and used as controls, and four wells were stretched. Two cover slips on each 4-well-plate were prepared as controls for immunostaining, since the first Flexcell®-experiment results showed autofluorescence on Uniflex-membranes. EB-culture medium was changed 3 times a week. Regimen used for stretching was the same as in the first experiment (Table 8). Proteins studied in this experiment were the following: cTnT, MyBP-C, α-actinin, connexin-43 and in the last time point also atrial and ventricular myosin light chains (MLC2a and MLC2v respectively).

### 4.4.3. The 3rd Flexcell®-experiment: UTA.06108.HCMM

The third Flexcell®-experiment was done using UTA.06108.HCMM cells (passage 18, age 20d). The time points were the same as in the previous experiment: 4, 7, 11 and 14 days. Total of 80 beating areas were cut, dissociated and plated on four Uniflex-plates and 8 coverslips on four 4-well-plates. On each Uniflex-plate, two wells were blocked with STOP-gums and used as controls, and four wells were stretched. Two cover slips on each 4-well-plate were prepared as controls for immunostaining. EB-culture medium was changed 3 times a week. Regimen used for stretching was altered a bit and is shown in table 9. Proteins studied in this experiment were the following: cTnT, MyBP-C, α-actinin, connexin-43, MLC2a, MLC2v, αTM and Ki-67.

**Table 9.** Regimen used in 3rd Flexcell® stretching on UTA.06108.HCMM.

| step | wave form | frequency (Hz) | elongation % | time |
|---|---|---|---|---|
| 1 | sin | 1 | 10 | 4, 7, 11 and 14d |

### 4.4.4. The 4th Flexcell®-experiment: UTA.07801.HCMM

Uniflex-membranes were pre-stretched for 24 hours before plating the dissociated CMs on them. Regimen for pre-stretching is shown in Table 10. Investigation of autofluorescense in Uniflex-membranes (lot#120313) showed that stretching the membrane decreased the level of autofluorescence shown in immunostainings. The fourth Flexcell®-experiment was done using UTA.07801.HCMM cells (passage 23, age 20d). The time points were 4, 7, 11 and 14 days. Total of 80 beating areas were cut, dissociated (buffer 2 incubation 70min) and plated on four Uniflex-plates and 8

coverslips on four 4-well-plates. On each Uniflex-plate, two wells were blocked with STOP-gums and used as controls, and four wells were stretched. Two cover slips on each 4-well-plate were prepared as controls for immunostaining. EB-culture medium was changed 3 times a week. Regimen used for stretching was altered and is shown in table 10. Proteins studied in this experiment were the following: cTnT, MyBP-C, α-actinin, MLC2a, MLC2v, αTM and Ki-67.

**Table 10.** Regimen used for pre stretching of Uniflex-membranes and 4th Flexcell®-stretching on UTA.07801.HCMM.

| step | wave form | frequency (Hz) | elongation % | time |
|---|---|---|---|---|
| 1 | sin | 1 | 7 | 4, 7, 11 and 14d |

### 4.4.5. The 5th Flexcell®-experiment: UTA.04602.WT

Uniflex-membranes were pre-stretched for 5 days before plating the dissociated CMs on them. Regimen for pre-stretching is shown in Table 10. The fifth Flexcell®-experiment was done using UTA.04602.WT cells (passage 29, age 20d). The time points were 4, 7, 11 and 14 days. Total of 88 beating areas were cut, dissociated and plated on four Uniflex- and coverslips on four 4-well-plates. On each Uniflex-plate, two wells were blocked with STOP-gums and used as controls, and four wells were stretched. Four cover slips on each 4-well-plate were prepared as controls for immunostaining. EB-culture medium was changed 3 times a week. Regimen used for stretching is shown in table 11. Proteins studied in this experiment were the following: cTnT, MyBP-C, α-actinin, MLC2a, MLC2v, αTM and Ki-67.

**Table 11.** Regimen used for 5th Flexcell®-experiment on UTA.04602.WT.

| step | wave form | frequency (Hz) | elongation % | time |
|---|---|---|---|---|
| 1 | sin | 0.5 | 3 | 3 min |
| 2 | sin | 0.5 | 5 | 5 min |
| 3 | sin | 1 | 7 | 4, 7, 11 and 14d |

## 4.5. Immunocytochemistry: double fluorescence staining protocol

All the steps in the double fluorescence staining protocol were performed for all samples on Uniflex -membranes and coverslips. After removing one Uniflex- and 4-

well-plate from the stretching experiment, EB-medium was aspirated and the samples were washed with 1xPBS (0.01M, pH7.4, Dulbecco's phosphate buffer saline, BE17-515F, Lonza) two times at RT for 5min. All the samples were fixed with 4% paraformaldehyde (PFA, Sigma-Aldrich) for 20min at room temperature (RT) as soon as possible (to prevent the effects of stretching from disappearing). PFA stored in 4°C was warmed to RT before applying. After fixation, the samples were washed two times with 1xPBS for 5min. Immunostainings were done immediately or samples were stored in PBS at +4°C for few days. Non-specific binding of the antibody was blocked and cells were permeabilized for 45 min at RT by using 10% NDS (normal donkey serum, Merck Millipore), 0.1% TritonX-100 (Sigma Aldrich), 1% BSA (Sigma Aldrich) in PBS. Samples were washed with 1% NDS, 0.1% TritonX-100, 1% BSA before adding primary antibody mixtures. Because of the large sample area of the Uniflex-membrane, Pap-Pen (G.Kisker, MKP-1) was used to border the application area of primary antibody mixtures for cost-efficiency. Total of five different primary antibody mixtures containing two primary antibodies (Table 12) produced in different animals were used: anti-cTnT and anti-MyBP-C, anti-cTnT and anti-α-actinin, anti-α-actinin and anti-connexin-43, anti-αTM and anti-Ki-67 (protein marker for cell division), anti-MLC2a and anti-MLC2v. Mixtures of primary antibodies were prepared in 1% NDS, 0.1% TritonX-100, 1% BSA in PBS. Primary antibodies were incubated on cells in +4°C overnight. On the next day, samples were washed three times with 1% BSA in PBS for 5min before applying secondary antibodies (Table 13). Alexa Fluor 488 and 568 were used in each mixture. Secondary antibody mixtures were prepared in 1% BSA in PBS. Pap-Pen was applied again on Uniflex-membranes to reinforce the bordering of the sample area. Samples were incubated in secondary antibody mixtures for 1hr in RT protected from light. To remove unbound antibodies, samples were washed three times with 1xPBS for 5min and two times with phosphate buffer working solution (0,01M, pH7.4) for 5min. The back of the Uniflex-membranes were washed to remove the silicone lubricant with 70% EtOH and by gently sweeping with cellulose paper. Sample areas from Uniflex-membranes were cut with scalpel and placed on 76x26mm microscope slides (Menzel-Gläser, Thermo Scientific) cells on top and mounted with Vectashield (Vector Laboratories Inc, H-1200), containing 49, 6-diamidino-2-phenylindole (DAPI) for staining nuclei, and thin 24x50mm microscope cover slips (Menzel-Gläser, Thermo Scientific). Coverslips containing control samples were dried in the

air and mounted on 76x26mm microscope slides with Vectashield and standard nail polish (edges only).

## 4.6. Imaging

Imaging of the immunostained samples was carried out with Zeiss AxioScope A1 fluorescent microscope and Zeiss AxioCam MRc5 camera. The microscope was operated with Zeiss' Zen 2012 software via PC. 10x, 20x, and 40x air objectives were used for imaging.

**Table 12.** Primary antibodies.

| Antibody | Origin | Dilution | Manufacturer |
|---|---|---|---|
| cTnT | goat IgG | 1:2000 | Abcam (ab64623) |
| MyBP-C | mouse IgG | 1:400 | Santa Cruz (sc-166081) |
| α-actinin | mouse IgG | 1:1500 | Sigma Aldrich (A7811) |
| Connexin 43 | rabbit IgG | 1:1000 | Sigma Aldrich (C6219) |
| MLC2a | mouse IgG | 1:200 | Synaptic Systems (311011) |
| MLC2v | rabbit IgG | 1:200 | Protein Tech (10906-1-AP) |
| αTM | mouse IgG | 1:200 | Santa Cruz (sc-73225) |
| Ki-67 | rabbit IgG | 1:600 | Millipore (AB9260) |

**Table 13.** Secondary antibodies.

| Antibody | Origin | Dilution | Manufacturer |
|---|---|---|---|
| Alexa Fluor 488 | donkey anti-mouse | 1:800 | Life Technologies (A21202) |
| Alexa Fluor 488 | donkey anti-rabbit | 1:800 | Life Technologies (A21206) |
| Alexa Fluor 568 | donkey anti-goat | 1:800 | Life Technologies (A11057) |
| Alexa Fluor 568 | goat anti-mouse | 1:800 | Life Technologies (A11004) |

## 4.7. Image analysis

Images from all three filters (DAPI, Alexa Fluor 488, Alexa Fluor 568) were stacked with Adobe Photoshop CS4. Proportions of Ki-67, MLC2a and MLC2v positive and negative cells were counted from single cells. Each individual sarcomere proteins' organization was analyzed from each image in which the protein was stained.

Structural organizations of proteins were categorized into three classes: disorganized (>75% of the protein disorganized or >50% punctuate expression), organized (protein organized or aligned >50% of the cell) and circular (protein localized circularly) (Figure 8). Alignment of single cells was analyzed with degree grid placed over the images with Adobe Photoshop CS4 (Figure 7). Cells aligned within +/– 45 degrees from the vertical 0° were categorized as vertical and cells aligned within +/- 44 degrees from the horizontal 0° were categorized as horizontal cells (Figure 7). Cells categorized as "others" were morphologically irregular, square in shape or round.

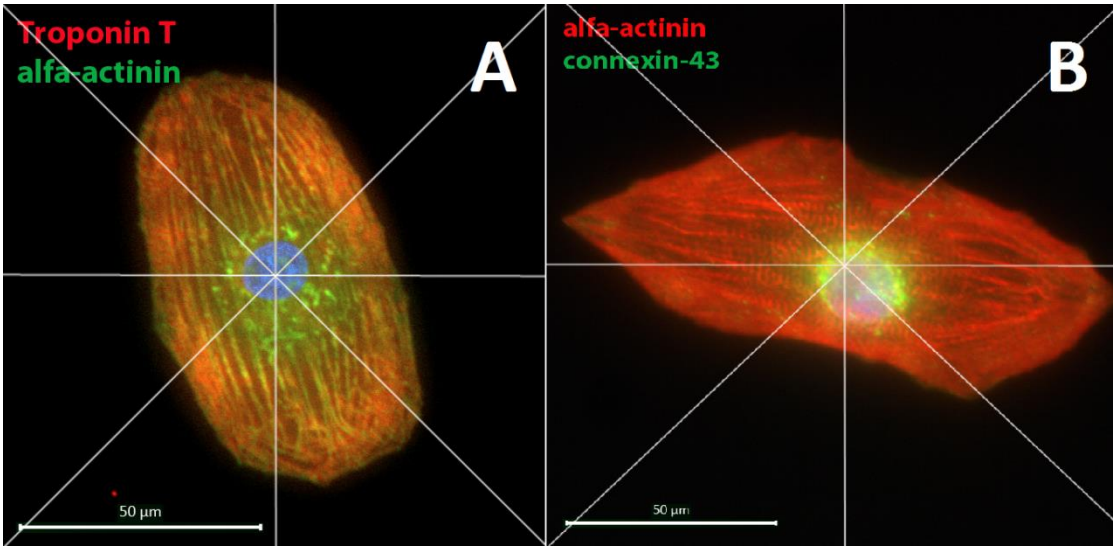


**Figure 7.** Degree grid used to determine the cell alignment from single cells in images. A = vertical, B = horizontal.

## 4.8. Statistical analysis

Error bars for the graphs were calculated as standard error of the mean (SEM), where

$$SEM = \frac{st.dev}{\sqrt{n}}$$

*st.dev* is standard deviation and *n* is the number of observations/samples. P-values were calculated using Chi-squared test with MS Excel.

## 4.9. Cell area analysis

Cell area analysis was done by collaborating researcher at University of Tampere, School of information sciences. A Matlab –based software was developed for this

purpose only, by Jyrki Rasku, PhD. All single cells were analysed from all immunostained images.

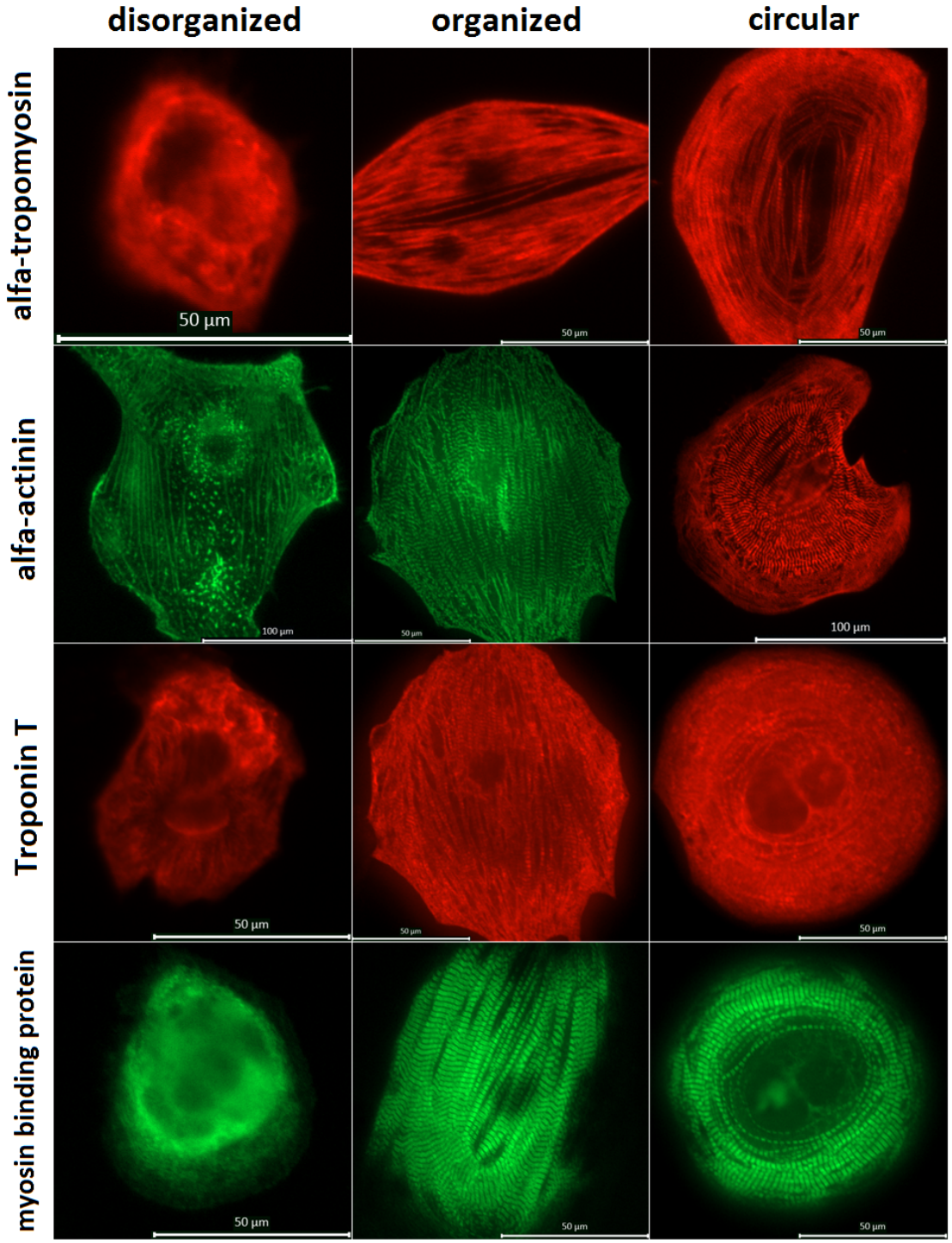


**Figure 8.** Examples of each four proteins (αTM, α-actinin, cTnT and MyBP-C) categorized into the three categories (disorganized, organized and circular).

# 5. Results

In this study, HCM –patient specific and WT hiPSC –derived CMs were stretched with Flexcell® and samples were stained using immunocytochemistry, imaged and analyzed. Stretched samples were compared with controls and HCM CMs with WT CMs. Examples of immunostained CMs are shown in Figure 9. Because of small n-values in some HCM cell line samples, in each analyze, results from each HCM cell line were combined to view their results as one population.

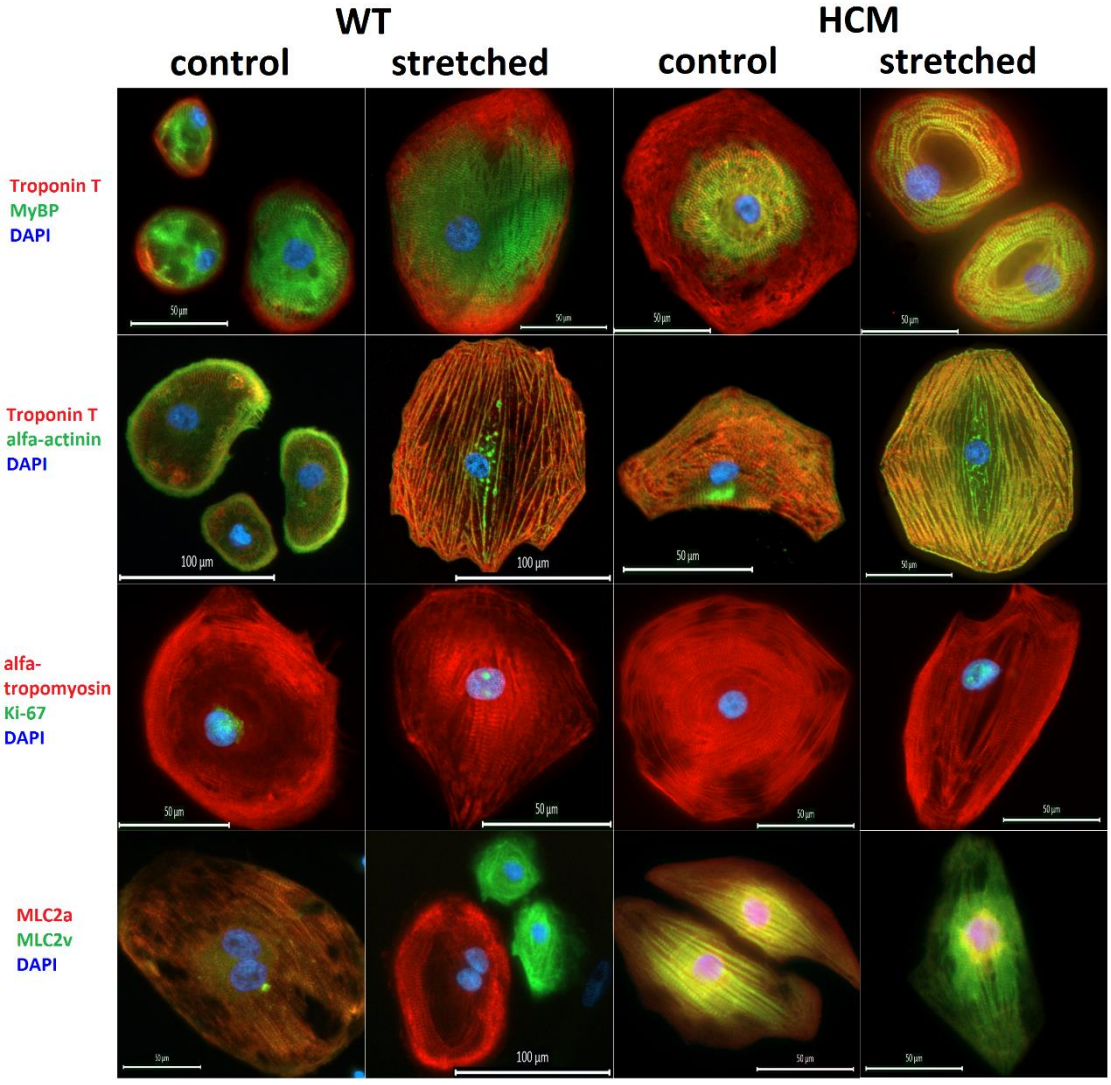


**Figure 9.** Examples of immunostained control and stretched WT and HCM cells.

## 5.1. Cell proliferation

Cell proliferation was studied in three cell lines: UTA.07801.HCMM, UTA.06108.HCMM and UTA.04602.WT (Figure 10). CMs were stained with anti-αTM and anti- Ki-67 primary antibodies. Ki-67 is a protein localizing in nucleus during interphase and it can be used as a cell division marker (Scholzen & Gerdes, 2000). Cells which expressed both proteins were counted as proliferating CMs. In UTA.07801.HCMM cell line, 52.5% (n=63) of control cells and 25.1% (n=141) of stretched cells were Ki-67 positive. The proliferation was relatively 52.2% lower in stretched than in control samples. In UTA.06108.HCMM cell line, the amount of proliferating cells was 73.1% (n=65) in control and 44.3% (n=316) in stretched samples. The proliferation was relatively 39.4% lower in stretched than in control samples. In UTA.04602.WT cell line, the amount of proliferating cells was 74.9% (n=101) in control and 53.2% (n=198) in stretched samples. The proliferation was relatively 29.0% lower in stretched than in control samples (Figure 10A). When comparing HCM and WT cells (Figure 10B), stretching decreases proliferation in both. Because of great SEM values, especially in stretched populations, it can not be said for sure how much HCM effects on cell proliferation.

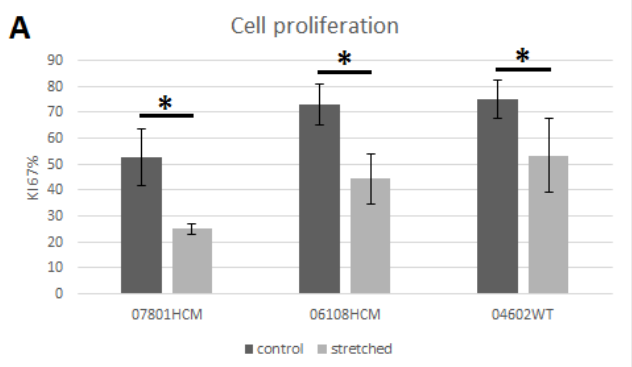


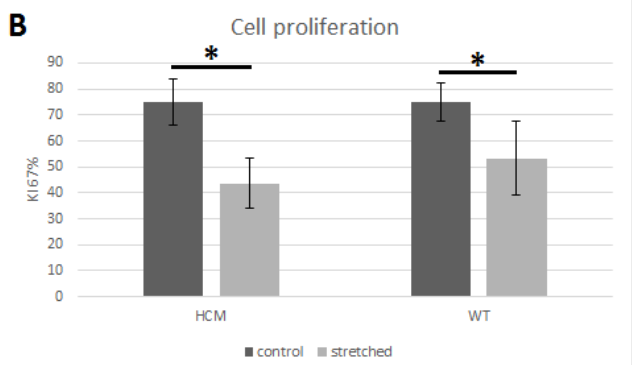


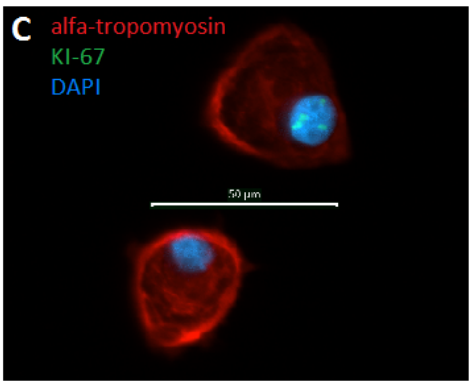


D

| Ki-67 positive cells | | |
|---|---|---|
| | controls | stretched |
| UTA.07801.HCM | 32 | 39 |
| UTA.06108.HCM | 43 | 135 |
| UTA.04602.WT | 71 | 101 |
| all HCM lines | 75 | 174 |

**Figure 10.** Cell proliferation. (A) Stretching decreases cell proliferation in all cell lines. (B) Stretching decreases cell proliferation in HCM and WT cells. (C) Example of Ki-67 positive and negative CMs. (D) Numbers of Ki-67 positive cells in control

and stretched samples for each cell line. (*) $p<0.002$. Error bars show standard error of the mean (SEM).

## 5.2. Sarcomere protein organization

In this study, organization of αTM (Figure 11), α-actinin (Figure 12), MyBP-C (Figure 13) and TnT (Figure 14) were analyzed. The results are presented for each individual cell line and as HCM and WT cells, where HCM cell lines are combined together. Statistically significant results were found.

Stretching increased 15.0% circular organization of αTM significantly in UTA.06108.HCMM cell line (Figure 11A). UTA.04602.WT cells responded to stretching by decrease of 27.4% in circular and increase of 33.7% in organized αTM structures (Figure 11C). When results from HCM cell lines were combined, no significant changes were found (Figure 11D).

Stretching increased 47.8% disorganized and decreased 50.0% organized structure of α-actinin significantly in UTA.05105HCMM cell line (Figure 12A). In UTA.04602.WT cell line, stretching significantly decreased 10.1% of circular and increased 14.8% disorganized structure of α-actinin (Figure 12D). When results from HCM cell lines were compiled, no significant changes were found (Figure 12E).

In UTA.07801.HCMM cell line, stretching significantly decreased 21.9% disorganized and increased 51.3% organized structure of MyBP-C (Figure 13B). In WT cells, significant decrease of 11.9% in circular MyBP-C organization was found (Figure 13D). When observing all HCM cells, significant decreases of 7.3% in disorganized and 0.8% in organized structures of MyBP-C was found (Figure 13E).

In UTA.07801.HCMM cell line, stretching significantly decreased 16.9% disorganized and increased 27.0% organized structure of TnT significantly (Figure 14C). In WT cells, all the structural organization changes of TnT induced by stretching were significant: 17.5% decrease in circular, 4.6% decrease in disorganized and 22.1% increase in organized structures were found (Figure 14D). In HCM cell population significant decrease of 3.8% was found in disorganized TnT structures after stretching (Figure 14E).

Differences in HCM and WT controls were studied statistically. Circular organization of αTM was significantly higher ($p=2.14\text{x}10^{-6}$), but organized structures were significantly lower in WT than HCM control cells ($p=8.25\text{x}10^{-6}$) (Figure 11D). Circular organization of α-actinin was significantly higher ($p=0.0052$), but

disorganized structures were significantly lower in control WT than control HCM cells (p=0.0016) (Figure 12E). There were significantly less disorganized structures of MyBP-C in WT than HCM control cells ($p=3.19x10^{-4}$) (Figure 13E). Circular organization of TnT was significantly higher (p=0.0012), but disorganized structures were significantly lower in WT than HCM control cells (p=0.0019) (Figure 14E). Also, there were significantly less disorganized structures of cTnT in WT than HCM control cells (p=0.0064) (Figure 14E).

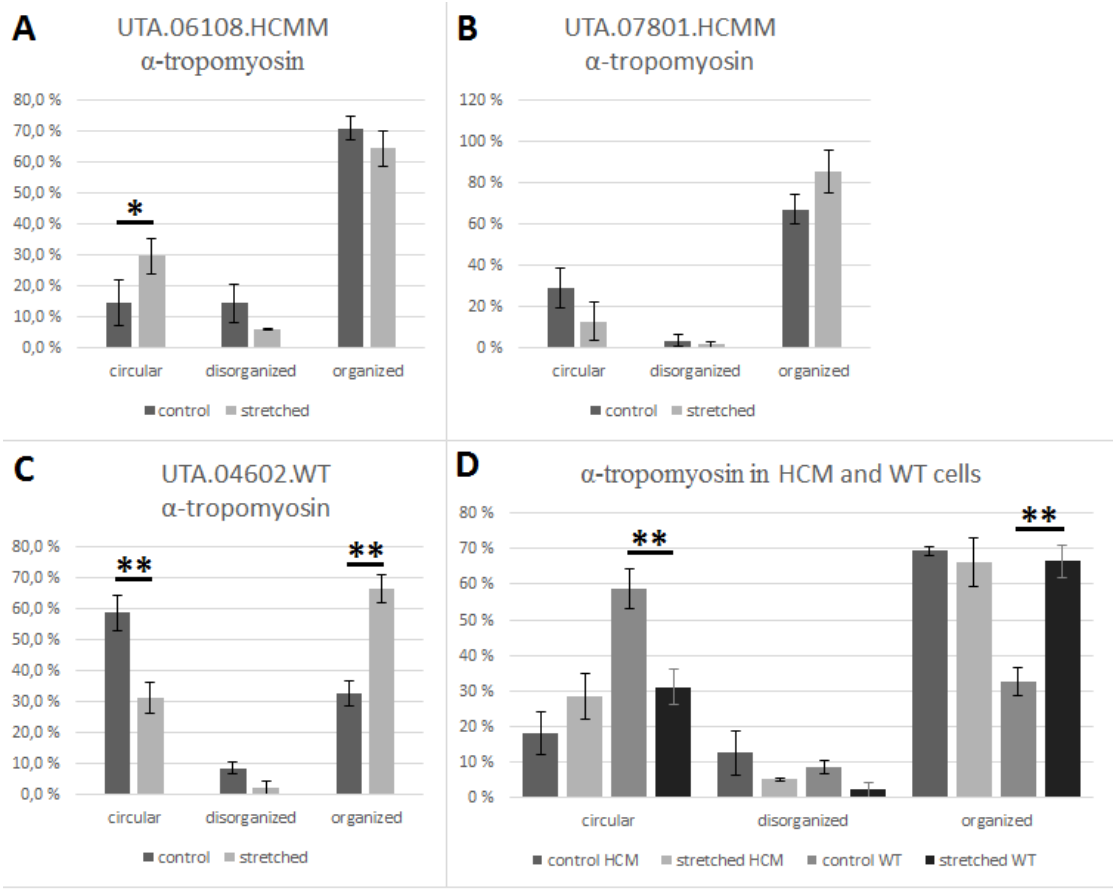


**E**

| alfa-tropomyosin | | circular | disorganized | organized | total |
|---|---|---|---|---|---|
| UTA.06108.HCM | controls | 5 | 5 | 29 | 39 |
| | stretched | 24 | 5 | 53 | 82 |
| UTA.07801.HCM | controls | 8 | 1 | 18 | 27 |
| | stretched | 7 | 1 | 27 | 35 |
| UTA.04602.WT | controls | 33 | 4 | 16 | 53 |
| | stretched | 33 | 4 | 73 | 110 |
| all HCM lines | controls | 13 | 6 | 47 | 66 |
| | stretched | 31 | 6 | 80 | 117 |

**Figure 11.** Alpha-tropomyosin organization. Organization of αTM (A-C) in each cell line. (D) HCM-cells compared to WT-cells. (E) Cell amounts in each category. (*) p<0.05, (**) p<0.01. Error bars show standard error of the mean (SEM).

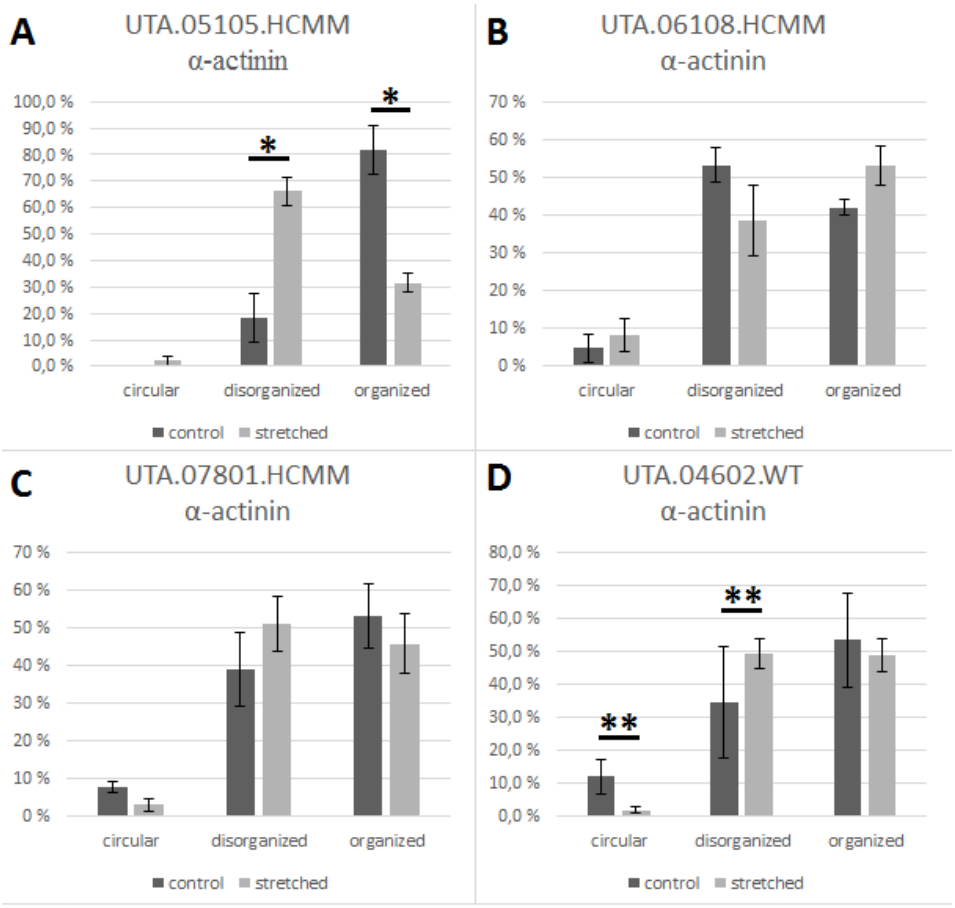


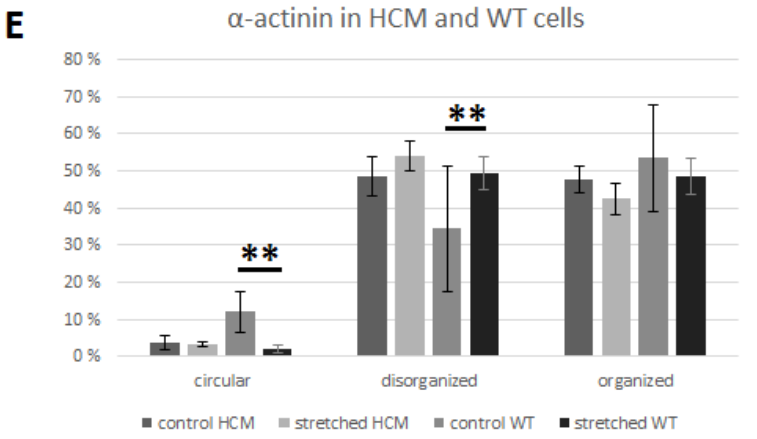


F

| alfa-actinin | | circular | disorganized | organized | total |
|---|---|---|---|---|---|
| UTA.05105.HCM | controls | 0 | 3 | 7 | 10 |
| | stretched | 1 | 41 | 19 | 61 |
| UTA.06108.HCM | controls | 1 | 47 | 34 | 82 |
| | stretched | 4 | 39 | 46 | 89 |
| UTA.07801.HCM | controls | 3 | 14 | 20 | 37 |
| | stretched | 2 | 32 | 36 | 70 |
| UTA.04602.WT | controls | 15 | 36 | 69 | 120 |
| | stretched | 4 | 62 | 57 | 123 |
| all HCM lines | controls | 4 | 64 | 61 | 129 |
| | stretched | 7 | 112 | 101 | 220 |

**Figure 12.** Alpha-actinin organization. (A-D) Organization of α-actinin in each cell line. (E) HCM-cells compared to WT-cells. (F) Cell amounts in each category. (*) $p<0.05$, (**) $p<0.01$. Error bars show standard error of the mean (SEM).

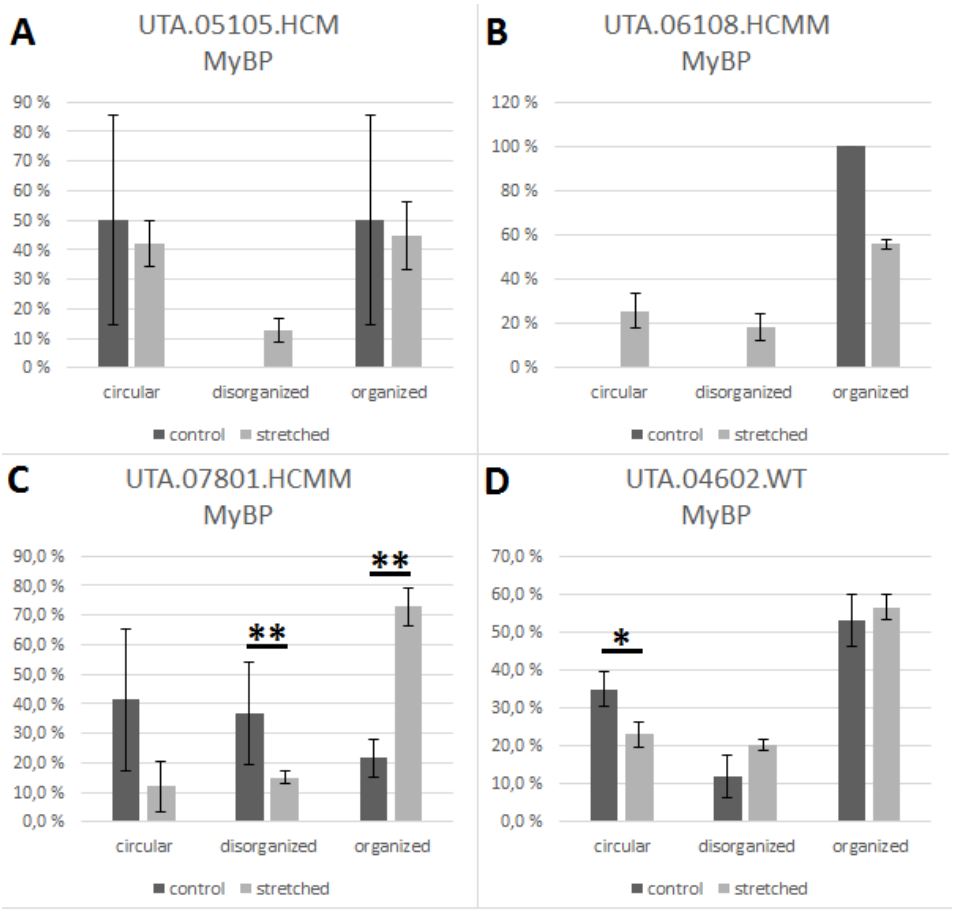


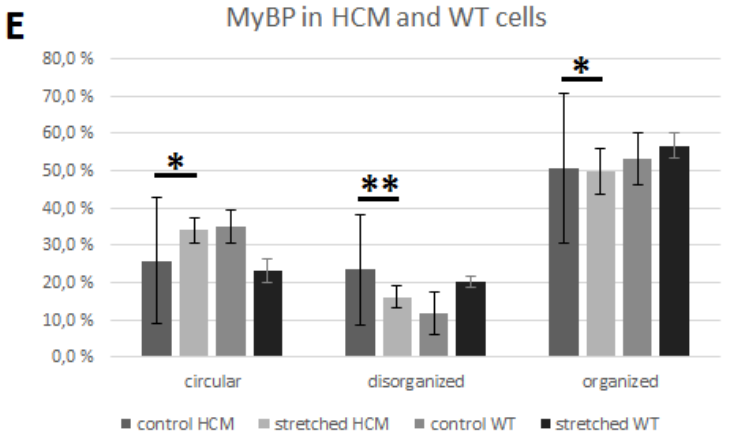


F

| MyBP | | circular | disorganized | organized | total |
|---|---|---|---|---|---|
| UTA.05105.HCM | controls | 1 | 0 | 1 | 2 |
| | stretched | 32 | 10 | 28 | 70 |
| UTA.06108.HCM | controls | 0 | 0 | 2 | 2 |
| | stretched | 15 | 10 | 32 | 57 |
| UTA.07801.HCM | controls | 8 | 17 | 9 | 34 |
| | stretched | 6 | 5 | 25 | 36 |
| UTA.04602.WT | controls | 45 | 22 | 64 | 131 |
| | stretched | 35 | 31 | 84 | 150 |
| all HCM lines | controls | 9 | 17 | 12 | 38 |
| | stretched | 53 | 25 | 85 | 163 |

**Figure 13.** Myosin binding protein C organization. (A-D) Organization of MyBP-C in each cell line. (E) HCM-cells compared to WT-cells. (F) Cell amounts in each category. (*) $p<0.05$, (**) $p<0.01$. Error bars show standard error of the mean (SEM).

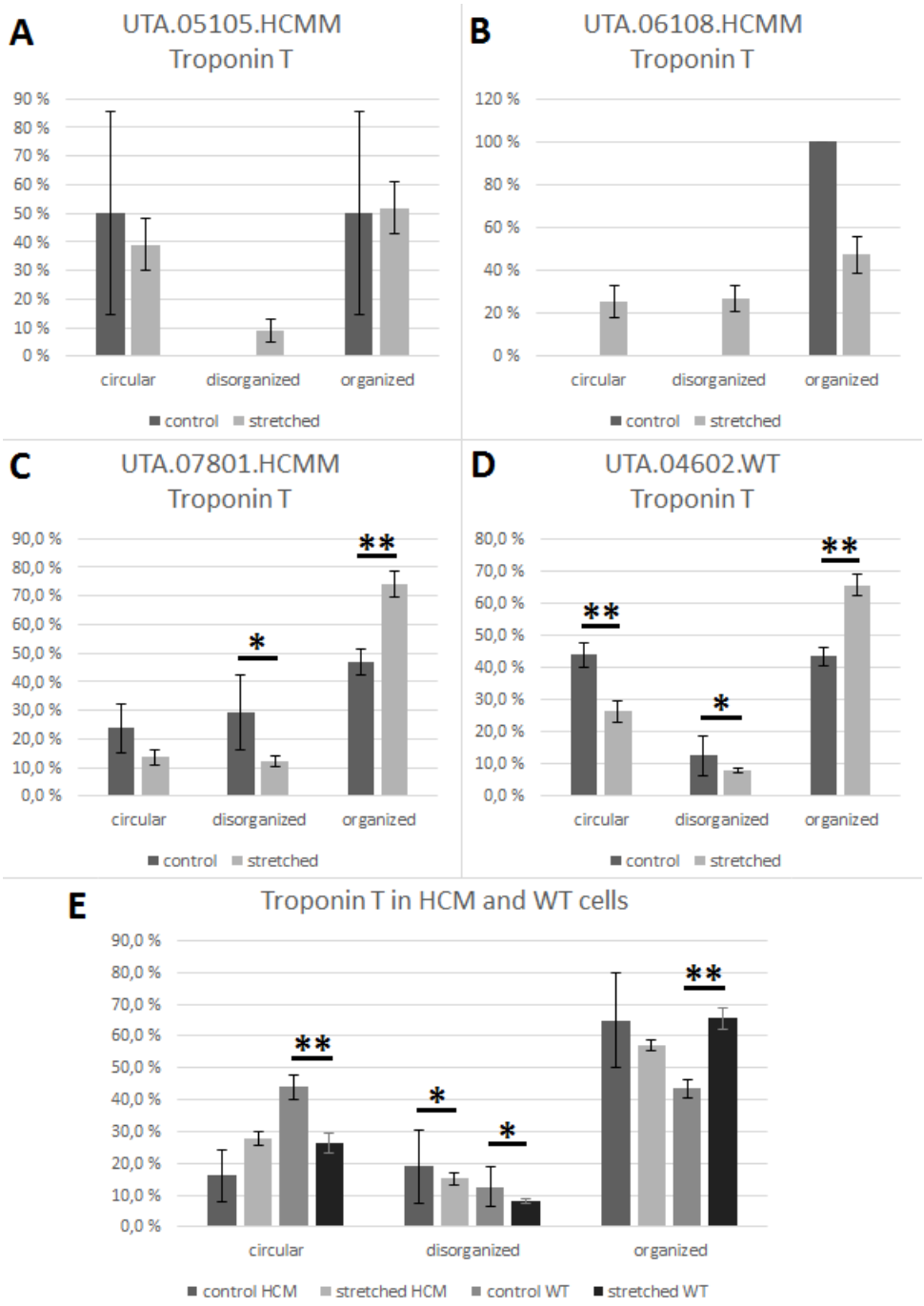


F

| Troponin T | | circular | disorganized | organized | total |
|---|---|---|---|---|---|
| UTA.05105.HCM | controls | 1 | 0 | 1 | 2 |
| | stretched | 33 | 9 | 37 | 79 |
| UTA.06108.HCM | controls | 0 | 0 | 2 | 2 |
| | stretched | 16 | 16 | 29 | 61 |
| UTA.07801.HCM | controls | 15 | 23 | 32 | 70 |
| | stretched | 17 | 14 | 77 | 108 |
| UTA.04602.WT | controls | 109 | 39 | 110 | 258 |
| | stretched | 84 | 25 | 194 | 303 |
| all HCM lines | controls | 16 | 23 | 35 | 74 |
| | stretched | 66 | 39 | 143 | 248 |

**Figure 14.** Troponin T organization. (A-D) Organization of TnT in each cell line. (E) HCM-cells compared to WT-cells. (F) Cell amounts in each category. (*) $p<0.05$, (**) $p<0.01$. Error bars show standard error of the mean (SEM).

## 5.3. Cell alignment

CMs from immunostained samples were categorized as vertical (alignment against the axis of strain) and horizontal (alignment along the axis of strain). Stretching significantly induced vertical alignment both in HCM and WT cells (Figure 15). In HCM cells, the increase was 21.4% (controls n=225, stretched n=518) compared to 24.3% (controls n=311, stretched n=413) in WT cells (Figure 15E). When studying individual cell lines, increases in vertical alignment were 16.8% (controls n=12, stretched n=141), 19.7% (controls n=111, stretched n=234), 30.2% (controls n=102, stretched n=143) and 24.2% (controls n=311, stretched n=413) in UTA.05105.HCMM, UTA.06108.HCMM, UTA.07801.HCM and UTA.04602.WT respectively (Figure 15A-D). In individual cell lines, decreases in horizontal alignment were 7.2% (controls n=12, stretched n=141), 17.9% (controls n=111, stretched n=234), 10.3% (controls n=102, stretched n=143) and 10.4% (controls n=311, stretched n=413) in UTA.05105.HCMM, UTA.06108.HCMM, UTA.07801.HCM and UTA.04602.WT respectively (Figure 15A-D). Trending of the effect of stretch over time to HCM and WT cells can be seen in Figure 16A-D. These results implicate that the uniaxial stretching increases vertical and decreases horizontal cell alignment in HCM and WT cell lines.

## 5.4. Multinuclearism

Multinuclearism was analyzed from each single CM by counting the amount of nuclei from images of immunostained samples (Figure 17). HCM and WT cells behave differently when it comes to multinuclear cell development (Figure 17A-B). HCM control cells develop increasing amounts of multiple nuclei during 2 weeks compared to stretched HCM cells, which keep the amount approximately the same. After 2 weeks of stretching, WT cells have approximately the same amount of multinuclear cells than in the beginning. However, total amount of multinuclear WT cells is less in stretched samples than controls because of the decreasing trend during until day 11. When comparing HCM and WT cells in general (Figure 17C), we see that in both there are less multinuclear cells in stretched samples. Also, there are less multinuclear cells in WT than HCM cells, 17.9% (n=381) versus 43.7% (n=295) in controls and 8.7% (n=554) versus 23.2% (n=767) in stretched samples. To conclude, HCM cells have more multinuclear cells than WT cells and stretching decreases the amount of

multinuclear cells significantly. There is significantly greater amount of multinuclear HCM than WT cells in control ($p=2.80x10^{-11}$) and stretched ($p=6.14x10^{-12}$) samples.

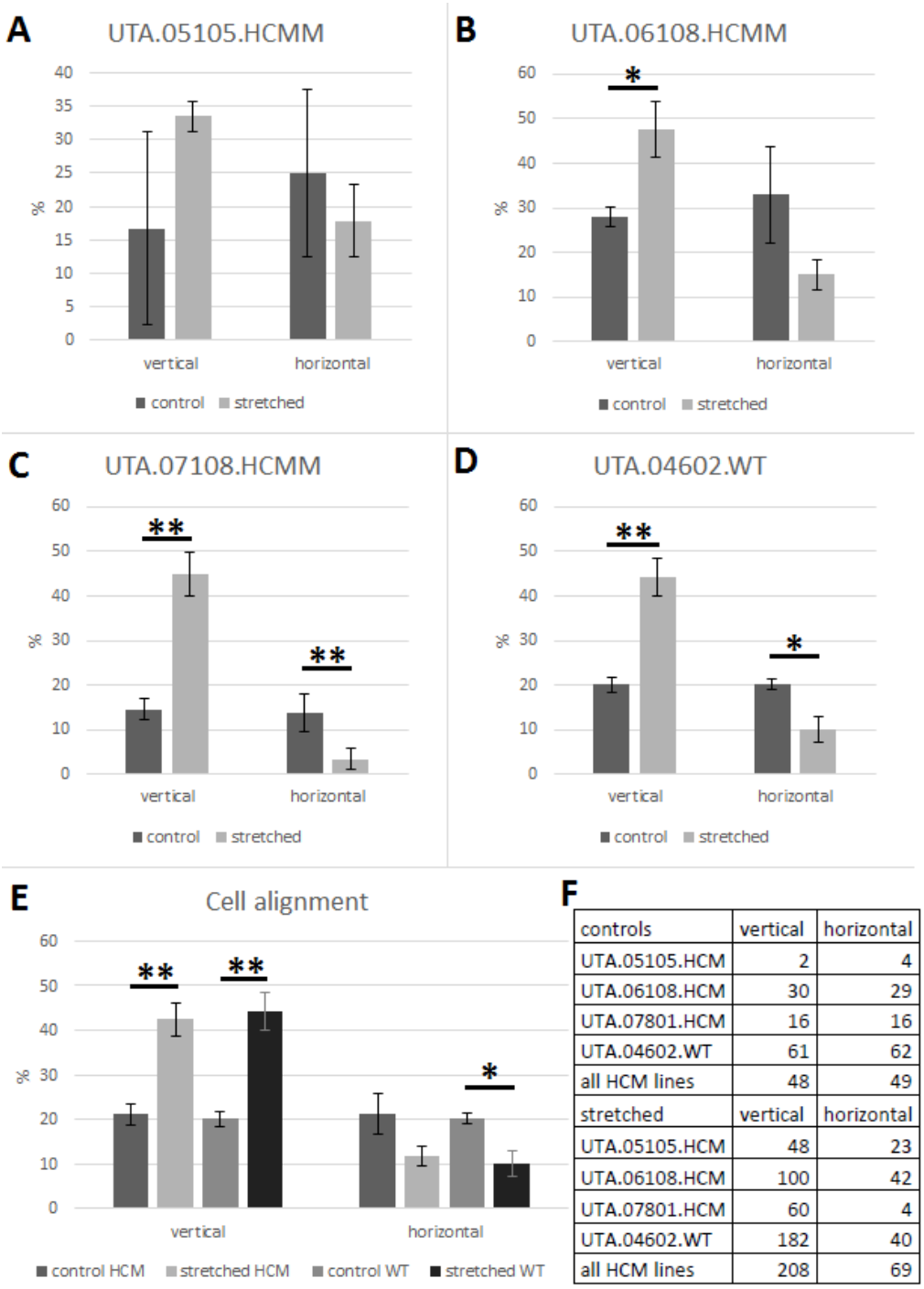


F

| controls | vertical | horizontal |
|---|---|---|
| UTA.05105.HCM | 2 | 4 |
| UTA.06108.HCM | 30 | 29 |
| UTA.07801.HCM | 16 | 16 |
| UTA.04602.WT | 61 | 62 |
| all HCM lines | 48 | 49 |
| stretched | vertical | horizontal |
| UTA.05105.HCM | 48 | 23 |
| UTA.06108.HCM | 100 | 42 |
| UTA.07801.HCM | 60 | 4 |
| UTA.04602.WT | 182 | 40 |
| all HCM lines | 208 | 69 |

**Figure 15.** Cell alignment. (A) No statistically significant differences in UTA.05105.HCMM –cell line. (B) Stretching significantly increases vertical alignment of UTA.06108.HCMM –cells. (C, D) Stretching significantly increasis vertical and decreases horizontal alignment in UTA.07801.HCMM- and UTA.04602.WT -cells. (E) Stretching significantly increases vertical alignment of both HCM and WT cells. (F) Amount of vertically and horizontally aligned cells in

each cell line. (*) p<0.05, (**) p<0.01.Error bars show standard error of the mean (SEM).

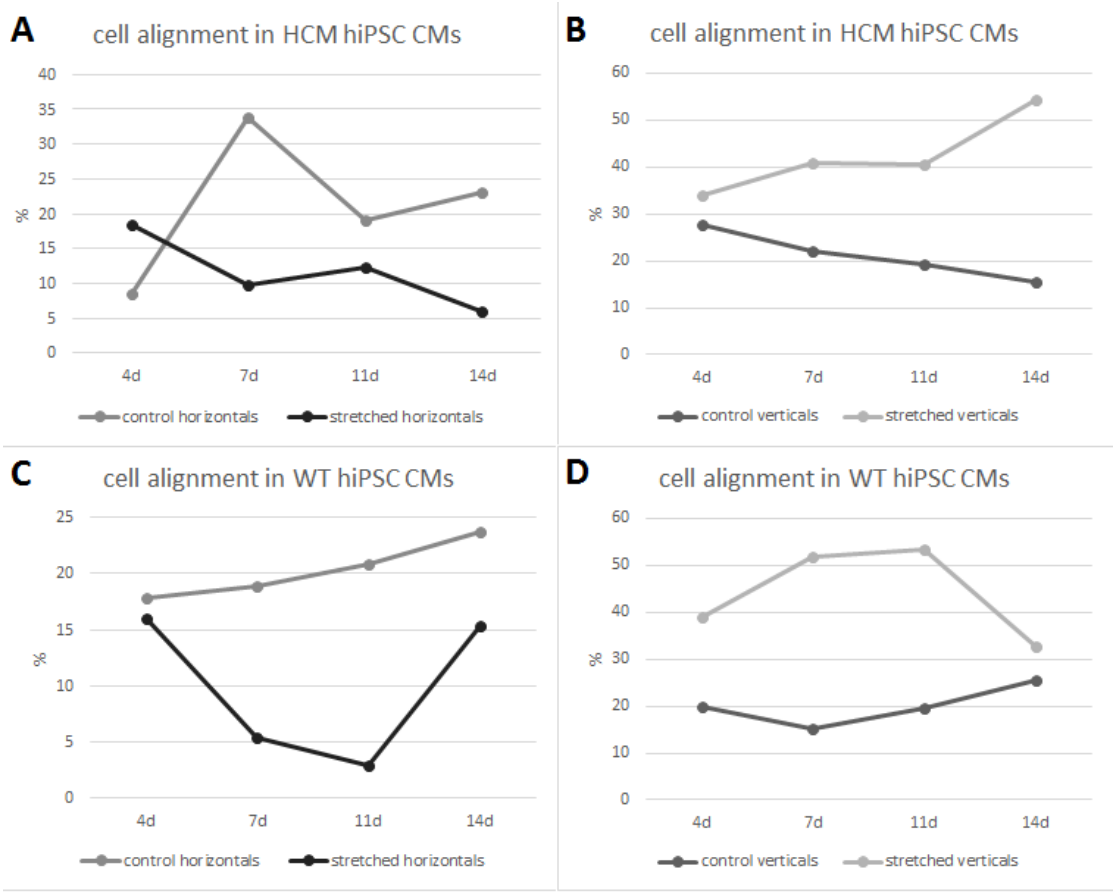


E

| | HCM | | WT | |
|---|---|---|---|---|
| | vertical | horizontal | vertical | horizontal |
| 4d control | 16 | 5 | 18 | 16 |
| 4d stretch | 72 | 39 | 27 | 11 |
| 7d control | 15 | 23 | 13 | 16 |
| 7d stretch | 42 | 10 | 58 | 6 |
| 11d control | 9 | 9 | 15 | 16 |
| 11d stretch | 49 | 15 | 54 | 3 |
| 14d control | 8 | 12 | 15 | 14 |
| 14d stretch | 45 | 5 | 43 | 20 |

**Figure 16.** Cell alignment at each time point. (A-D) Effect of stretching over time on HCM and WT cell alignment. (E) Amounts of vertical and horizontal aligned cells in each time point.

## 5.5. Atrial and ventricular cardiomyocytes

Percentages of MLC2a- and MLC2v -positive single CMs were calculated from images of immunostained samples. Ventricular adult CMs express both atrial and ventricular myosin light chains (Bird et al., 2003). Cells which expressed only MLC2a

were counted as atrial- and the rest expressing both or only MLC2v as ventricular CMs. In stretched samples, there were more atrial CMs than in control samples (Figure 18). In control HCM cells (n=109), there were no atrial CMs at all compared to the stretched HCM cells (n=177) in which there were 26.8%. In control WT cells (n=66), there were 3.0% and in stretched WT cells (n=48) 12.5% atrial CMs. All in all, there were more ventricular CMs in each sample.

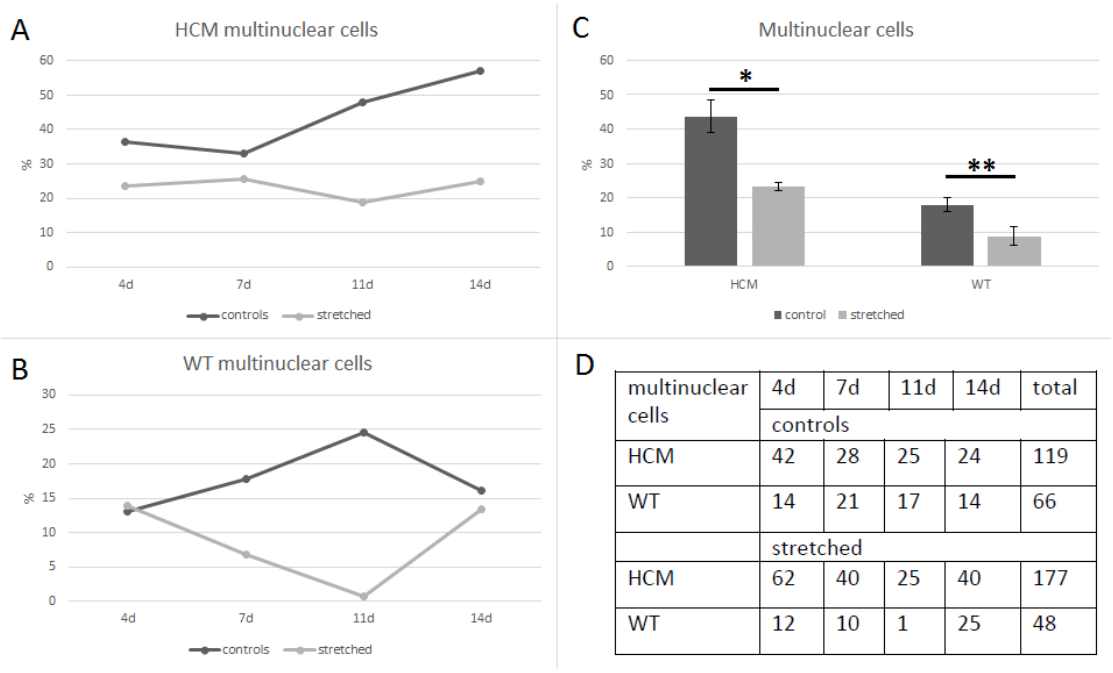


D

| multinuclear cells | 4d | 7d | 11d | 14d | total |
|---|---|---|---|---|---|
| | controls | | | | |
| HCM | 42 | 28 | 25 | 24 | 119 |
| WT | 14 | 21 | 17 | 14 | 66 |
| | stretched | | | | |
| HCM | 62 | 40 | 25 | 40 | 177 |
| WT | 12 | 10 | 1 | 25 | 48 |

**Figure 17.** (C) Percentages of multinuclear cells in HCM and WT cells. Percentages of multinuclear cells in HCM (A) and WT (B) cells in each time point. (D) Multinuclear HCM and WT cells in control and stretched samples. (*) $p=1.91x10^{-8}$, (**) $p=7.01x10^{-5}$. Error bars show standard error of the mean (SEM).

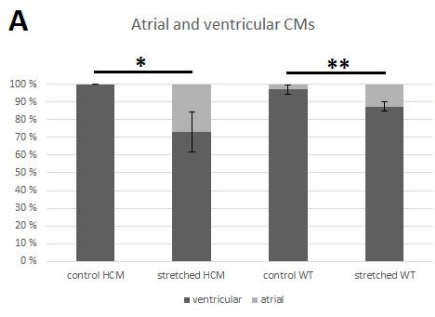


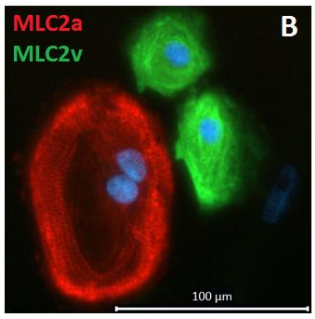


C

| HCM | atrial | ventricular |
|---|---|---|
| controls | 0 | 56 |
| stretched | 99 | 195 |
| WT | atrial | ventricular |
| controls | 3 | 94 |
| stretched | 25 | 149 |

**Figure 18.** Atrial and ventricular cardiomyocytes in HCM and WT cells. (A) Percentages of atrial and ventricular CMs in control and stretched HCM and WT cells. (B) Example of atrial (red) and ventricular (green/red) CMs. (C) Amounts of the cells. (*) $p=2.93x10^{-7}$, (**) $p=0.0035$. Error bars show standard error of the mean (SEM).

## 5.6. Cell area

Cell areas were calculated from all four cell lines used in this study. Only single CMs' cell areas were analyzed. Stretching increased cell area in WT cells 74.1-88.8% throughout the two weeks of stretching (Figure 19A). Stretching induced cell area growth faster during the first week of stretching in HCM cells, but in the end, the control HCM cells were 10.0% bigger than stretched HCM cells (Figure 19A). Control HCM cells were bigger than control WT cells. In the end of two weeks of stretching, HCM cells were 19.0% bigger than WT cells.

A

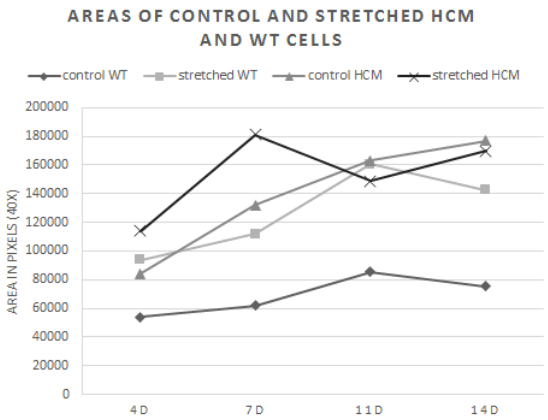


B

| WT | | | |
|---|---|---|---|
| sample | average area (px) | n | stretched/control |
| 4d control | 53800,41 | 114 | 1,740935 |
| 4d stretched | 93663,03 | 75 | |
| 7d control | 61775,72 | 129 | 1,809758 |
| 7d stretched | 111799,1 | 89 | |
| 11d control | 85229,37 | 59 | 1,88603 |
| 11d stretched | 160745,2 | 83 | |
| 14d control | 75544 | 62 | 1,887803 |
| 14d stretched | 142612,2 | 104 | |

| HCM | | | |
|---|---|---|---|
| sample | average area (px) | n | stretched/control |
| 4d control | 84085,57 | 54 | 1,355509 |
| 4d stretched | 113978,7 | 182 | |
| 7d control | 131804,8 | 60 | 1,373578 |
| 7d stretched | 181044,1 | 93 | |
| 11d control | 163062,4 | 34 | 0,91246 |
| 11d stretched | 148787,9 | 101 | |
| 14d control | 176724,4 | 16 | 0,960254 |
| 14d stretched | 169700,3 | 71 | |

**Figure 19.** (A) Average areas of the cells in each time point in WT and HCM cell lines. (B) Tables showing the values in graph, amount of cells in each sample and ratios of stretched/control average cell areas.

# 6. Discussion

## 6.1. Study setup

In most publications in which Flexcell® has been applied, murine CMs have been used, so this study with hiPSCs was somewhat novel in nature. The longest stretching periods in earlier publications using murine CMs was only 2 days (Boateng et al., 2006; de Jonge et al., 2002; Facundo et al., 2012). In this study the longest stretching period was 2 weeks. With this kind of dramatic increase in stretching time period, added to that hiPSCs –derived CMs were used, the hopes of finding something new were high. The HCM patient specific hiPSC derived CMs with the mutation in *MYBPC3* used in this study offer a great model to study different aspects of the disease.

One of the most important step in the study was the dissociation of the CMs. First of all, the trickiest part of dissociation is the up and down pipetting of the aggregate solution trying to get single cells. Depending on the cutting of the beating areas, there are various sizes of aggregates from which some are tougher than others. This step affects the survivability of the cells and the starting material volume greatly, since if the cells are handled too hard, they may be damaged and do not start growing and proliferating after plating. The 2$^{nd}$ buffer incubation time in dissociation protocol was slightly increased from 45 minutes to one hour making aggregates dissociate better. It was noticed during this study, that the success of dissociation was greater in the last experiment than in the first one, resulting in more cells in the samples.

## 6.2. Flexcell®

The Flexcell® –apparatus was not well known in the research group before this study. There were some practical and technical issues along the study which more or less made things difficult. First of all, the controller unit is very prone to get damaged. While the compressor pump is operating, the tubes in which the air flows, condensate moisture over time. If the moisture reaches the controller unit, the sensors which measure the pressure, and regulate the elongation-% of the membrane, become dysfunctional. This leads to inappropriate pressure output of the pump and loss of function of the stretching. This happened during this study and it created a delay in

the process because the controller unit had to be sent for repair. After the repair, additional filter was added between the tubing and the controller unit to capture the moisture and preventing it reaching the electronics of the sensors. Secondly, during the whole study, the displayed elongation-% was never the same as the input in the operating software. The input in the regimen had to be increased in order to get the elongation-% that was wanted. In the regimen tables of this thesis, the elongation percentages are the ones displayed by the software. Also, the Flexcell® International Corporation Culture Plate & Loading Station™ User's Manual sets the maximum elongation-% sustained by the Flexcell® to 12.2% which is about 90 kPa provided by the pump. In first experiments, a higher elongation-% of 10% was used, but it unfortunately was one reason behind the controller unit malfunction. It was concluded that stretching of 2 weeks with that high pressure, makes the moisture condensate more rapidly.

More severe problems was created by the autofluorescence of the Uniflex-membranes. It was noticed after the first experiments that using the STOP-gums for creation of control (non-stretched) samples resulted in huge amount of autofluorescence which affected the images negatively. Also slighter amount of autofluorescence was noticed in some stretched Uniflex-membranes too. Throughout the study 21 of 104 samples were unable to be imaged because of the autofluorescence. During the first experiment there was no autofluorescence because higher elongation-% (10%) was used. After the controller unit repair, the elongation-% was dropped to 7% which resulted in increased autofluorescence in samples. It was decided to try to fix the problem with pre-stretching the Uniflex-membranes before plating the cells. Apparently, the 10% elongation during pre-stretching is more effective removing the autofluorescence than 7% elongation.

## 6.3. Immunostainings

Exceptionally, older anti-connexin-43 primary antibody was probably used staining the 11d and 14d time point samples in 3$^{rd}$ Flexcell®-experiment with UTA.06108.HCMM cell line, resulting to failed staining. The connexin-43 was not included in any analyses and was replaced by other antibody combination in later experiments.

Cells stained with primary antibody for Ki-67 were analyzed for cell proliferation. Ki-67 is a cell division marker which is localized exclusively within the nucleus during interphase and on the surface of chromosomes during mitosis (Scholzen & Gerdes, 2000). It is present in all active cell cycle phases, leaving resting cells unstained. Even though the phases of the cell cycle could be, in at least some extent, determined by analyzing the localization pattern of Ki-67 within the nucleus, in this the focus was on the presence of the protein in the nuclei and it was used as a proliferation marker only.

In three cell lines (UTA.06108.HCMM, UTA.07801.HCMM and UTA.04602.WT), cells were stained with anti-MLC2a and anti-MLC2v primary antibodies to distinguish atrial and ventricular CMs from each other. Surprisingly, some cells showed binding of both MLC2a and MLC2v antibodies to the same cell. This was thought to be a consequence of nonspecific binding of the antibodies or cells being immature. Interestingly, it has been shown earlier that ventricular adult CMs, obtained from human biopsies, express both atrial and ventricular myosin light chains (Bird et al., 2003). It may be possible that in disease state like HCM, this kind of expression takes place (Cummins, 1982). The results suggest that hiPSC derived ventricular CMs also express both MLC2a and MLC2v. There were very few atrial CMs in control samples. The results suggest that stretching increases the amount of atrial CMs. This could provide a novel strategy for development of more mature tissue crafts in the future, with more even ratio of atrial and ventricular CMs in them.

## 6.4. Effects of uniaxial strain on hiPSC –derived CMs

Cell proliferation was lower in stretched samples than in control samples suggesting that the mechanical stress was too much for the cells. In some images taken from stretched samples, there were parts of broken cells visible. Surprisingly, the proliferation was higher in UTA.06108.HCMM cells than in UTA.07801.HCMM cells even though the mechanical stress during the stretching was higher (elongation-% 10% and 7% respectively). On the other hand, hiPSC derived CMs maturate over time in culture and should resemble more the mature adult CM phenotype which is known to proliferate very little if at all (Robertson et al., 2013).

Organizational analysis of each stained sarcomere protein did not reveal consistent patterns of behavior of sarcomere structure under mechanical stress. Each

CM's individual state of maturity, affecting the cell morphology, could be even more major factor in the organization of sarcomeres in these cells than the stretching. Immature CMs are usually round whereas more mature CMs are square, longitudinal or irregular in shape (Robertson et al., 2013). From the four analyzed sarcomere proteins, α-actinin and MyBP-C showed interesting features in some CMs. There were punctuate α-actinin structures in some CMs, which were categorized in the disorganized category. This could be caused by excessive amount of mechanical stress to the cells, leading to a breaking of α-actinin connections between sarcomere units. Similar punctuate behavior of α-actinin have been reported earlier in DCM - patient specific hiPSCs (Sun et al., 2012).

Organization of MyBP-C was the biggest question since the HCM cell lines used in this study had the *MYBPC3* Finnish founder mutation in them. Surprisingly, from the immunostained images, it was noticed that the expression of MyBP-C was incomplete throughout some cells, some even lacking it completely. This was observed both in HCM and WT cells, even in control samples. The MyBP-C lacking cells still stained positive for cTnT which identified them as CMs. Possibilities for this kind of incomplete staining/expression of MyBP-C in these cells could be caused by malfunction of the anti- MyBP-C primary antibody, variation in CM permeability for antibodies or sarcomere protein turnover in CMs. The primary antibody function could be tested by using another one for comparison and the permeability of CMs could be increased by increasing concentration of TritonX-100 in staining protocol. Theory about MyBP-C turnover needs further investigation, still it could be possible that the truncated MyBP-C has increased degradation rate and only the newly synthetized protein in the proximity of nucleus becomes stained (Figure 9). However, WT cells, which are supposed to have perfectly normal MyBP-C structure, showed same kind of expression in immunostained images. Interactions between actin and MyBP-C are essential for maintenance of sarcomere assembly: MyBP-C without actin binding domain was shown to be stable but with limited incorporation into sarcomere structure, whereas cardiac dysfunction was observed with disrupted MyBP-C – actin interaction (Bhuiyan et al., 2012; Kulikovskaya et al., 2003). One reason for interruption of MyBP-C – actin interactions could be stress overload. Under cardio- and cytotoxic conditions, carbonylation and degradation of MyBP-C was observed (Aryal et al., 2014).

One of the hypotheses in the beginning of the study was that the uniaxial stretching could be used to align cells in desirable fashion. Parallel alignment of CMs is an important factor for the synchronous function in living tissue (Bers 2001; Severs, 2000). If cells could be aligned in preferred manner, it could improve the maturation of the cells and help creating more authentic and functional tissue crafts in the future (Lundy et al., 2013). The results implicate that the cells tend to align across the axis of uniaxial strain.

There were more multinuclear cells in control samples than stretched samples and in HCM than WT cells. Results suggest that stretching decreases the amount of multinuclear cells. Mature adult CMs are usually bi- or multinucleated because of the lack of cytokinesis after embryonic development and birth (Clubb & Bishop, 1984, Robertson et al., 2013). It has been thought that polyploidization is caused by a special cellular program that protects the cells from uncontrolled proliferation or apoptosis (Storchova & Pellman, 2004). This kind of program is thought to protect the working myocardium and enable CMs to adapt to disease condition such as in hypertrophic growth (Liu et al., 2010).

Interesting results were obtained from cell area analysis: control WT cells are smaller than control HCM cells and stretching increases WT cell area greatly compared to HCM cells after two weeks of stretching. Since HCM cells are bigger than WT cells to begin with, the change in cell area is greater in WT cells. As described earlier, mechanotransduction in CMs can lead to activation of growth signals (Sadoshima and Izumo, 1997). HCM cells may have already, because of the disease caused by gene mutation in sarcomeric protein leading to altered cell function, accommodated themselves to a state in which the cell size is bigger.

All the analyses presented here were based on looking into single cells in the samples. However, because of the method how cells were processed before plating, there were cell aggregates in samples also. No quantitative analysis were made but two different observations were noticed: first, the cell clumps tended to scatter in the stretched samples. It could be a consequence of the excessive force of stretching, which resulted tearing the cells apart. The scattered cells next to each other showed puzzle –like morphology, which indicated that they might have been in close cell-to-cell connections with each other. Second, the cell clumps seemed to be more normal in sarcomere structure than single cells in general. This may be a result of gap junctions formed between CMs by connexins, which allows signaling between the

cells. The signaling between cells may lead to compensatory effects. Same kind of behavior was reported earlier in DCM patient specific hiPSCs (Sun et al., 2012).

## 6.5. hiPSCs as a disease model

hiPSCs offer an easier setup of disease modeling and drug screening than ESCs and do not have the ethical issues. One of the benefits with hiPSCs is the opportunity to create controls from the same patient by "curing" a mutation which allows use of relevant controls with the same ethnic genotype, known as isogenic controls (Soldner et al., 2011). This kind of setup allows experiments to be performed under genetically defined conditions. Eventually, hiPSCs may reduce use of animal models. Working with animal models is expensive and the data obtained from animal studies do not always reflect the outcome in humans. However, there are some issues considering hiPSCs authenticity, such as immaturity and incomplete penetrance of the disease being modeled, leading to different phenotypes with same mutations (Bellin et al., 2012). On the other hand, this kind of behavior can be considered as an opportunity to study the effect of background and epigenetics.

hiPSC derived CMs are structurally and functionally immature and they have fetal-like properties (Keung et al., 2014; Robertson et al., 2013). The maturation seems to depend greatly on the cultivation time in culture and also culture conditions and method of differentiation (Keung et al., 2014; Lundy et al., 2013; Robertson et al., 2013). hiPSC CMs exhibit different morphologies, structure, proliferation, gene expression, metabolism, bioenergetics, electrophysiological properties and calcium handling (Robertson et al., 2013).

Systematic quantification of similarities and differences in hiPSC derived CMs and adult CMs is complicated because of the fact that different studies use diverse methods, culture conditions and cell lines of origins. CM differentiation from hiPSCs takes advantage of co-culturing with other cells and various culture conditions. The type of differentiation has effects on the outcome of CM maturation but the exact mechanisms are poorly known. With various differentiation methods, CMs with different properties are acquired. CMs differentiate further into atrial-, ventricular- and pacemaker –cells, which are obtained in different proportions depending on differentiation method (Robertson et al., 2013). Unfortunately, the effectiveness of CM differentiation methods are still very low. Individual research groups, though,

may have their own adjustments and tweaks to differentiation methods and protocols. This kind of constant developing and studying of the protocols hopefully leads to a more effective differentiation methods in the future. Also, different surface materials can have an effect on the morphology and maturity of the cells. Studies have been carried out by testing different topographical surfaces for cell culturing in 2D and 3D models (Bian et al., 2014; Liau et al., 2011; Rao et al., 2013).

# 7. Conclusions

In this study, effects of uniaxial mechanical strain on HCM –patient specific and control hiPSC –derived CMs were studied. Mechanical uniaxial stretching of HCM -patient specific and control hiPSC -derived CMs decreases cell proliferation, has effects on sarcomere protein organization, increases alignment against the axis of the strain, decreases multinuclearism, increases proportion of atrial cardiomyocytes in culture and increases wild type cells' size.

In the future, more studies of the functionality, morphology and maturity of hiPSC –derived CMs are needed to discover the true potential of hiPSC –applications in cardiac disease modeling. The immaturity of hiPSC –derived CMs yet restrict their use in clinical applications. More effective differentiation methods, tissue engineering studies and advanced culturing conditions are needed to provide new strategies to develop more mature hiPSC –derived CMs for cardiac regenerative medicine.

# 8. References

Alders M, Jongbloed R, Deelen W, van den Wijngaard A, Doevendans P, Ten Cate F, et al. The 2373insG mutation in the MYBPC3 gene is a founder mutation, which accounts for nearly one-fourth of the HCM cases in the Netherlands. Eur Heart J . 2003;24:1848 – 53.

Anderson ME, Brown JH, Bers DM. CaMKII in myocardial hypertrophy and heart failure. J Mol Cell Cardiol. 2011;51(4):468-73.

Aryal B, Jeong J, Rao VA. Doxorubicin-induced carbonylation and degradation of cardiac myosin binding protein C promote cardiotoxicity. Proc Natl Acad Sci U S A. 2014;111(5):2011-6.

Ashrafian H, Redwood C, Blair E, Watkins H. Hypertrophic cardiomyopathy: a paradigm for myocardial energy depletion. Trends Genet. 2003;19(5):263-8.

Ayettey AS, Navaratnam V. The T-tubule system in the specialized and general myocardium of the rat. J Anat. 1978;127(1):125-40.

Barefield D, Kumar M, de Tombe PP, Sadayappan S. Contractile dysfunction in a mouse model expressing a heterozygous MYBPC3 mutation associated with hypertrophic cardiomyopathy. Am J Physiol Heart Circ Physiol. 2014;306(6):807-15.

Bellin M, Marchetto MC, Gage FH, Mummery CL. Induced pluripotent stem cells: the new patient? Nature Reviews Molecular Cell Biology 2012;13:713-726.

Bers DM. Calcium Cycling and Signaling in Cardiac Myocytes. Annu. Rev. Physiol. 2008. 70:23–49

Bers DM. Calcium Fluxes Involved in Control of Cardiac Myocyte Contraction. Circ Res. 2000;87:275-281.

Bers DM. Excitation-contraction coupling and cardiac contractile force. 2nd edition, Kluwer academic publishers, Dordrecht, 2001.

Bhuiyan MS, Gulick J, Osinska H, Gupta M, Robbins J. Determination of the critical residues responsible for cardiac myosin binding protein C's interactions. J Mol Cell Cardiol. 2012;53(6):838-47.

Bian W, Jackman CP, Bursac N. Controlling the structural and functional anisotropy of engineered cardiac tissues. Biofabrication. 2014;6(2):024109.

Bird SD, Doevendans PA, van Roojien MA, Brutel de la Riviere A, Hassink RJ et al. The human adult cardiomyocyte phenotype. Cardiovascular Research 2003;58:423–434.

Boateng SY, Belin RJ, Geenen DL, Margulies KB, Martin JL, Hoshijima M et al. Cardiac dysfunction and heart failure are associated with abnormalities in the

subcellular distribution and amounts of oligomeric muscle LIM protein. Am J Physiol Heart Circ Physiol. 2007;292(1):H259-69.

Bootman MD, Higazi DR, Coombes S, Roderick HL. Calcium signalling during excitation-contraction coupling in mammalian atrial myocytes. J Cell Sci. 2006;119(19):3915-25.

Bos JM, Towbin JA, Ackerman MJ. Diagnostic, prognostic, and therapeutic implications of genetic testing for hypertrophic cardiomyopathy. J Am Coll Cardiol. 2009;54(3):201-11.

Bowling N, Walsh RA, Song G, Estridge T, Sandusky GE et al. Increased protein kinase C activity and expression of Ca2+-sensitive isoforms in the failing human heart. Circulation. 1999;99(3):384-91.

Brodde OE, Michel MC. Adrenergic and Muscarinic Receptors in the Human Heart. Pharmacol Rev. 1999;51(4):651-90.

Bush EW, McKinsey TA. Protein acetylation in the cardiorenal axis: the promise of histone deacetylase inhibitors. Circ Res. 2010;106(2):272-84.

Chen CS. Mechanotransduction - a field pulling together? J Cell Sci. 2008;121(20):3285-92.

Chen-Izu Y, McCulle SL, Ward CW, Soeller C, Allen BM, Rabang C et al. Three-dimensional distribution of ryanodine receptor clusters in cardiac myocytes. Biophys J. 2006;91(1):1-13.

Chiu C, Bagnall RD, Ingles J, Yeates L, Kennerson M. Mutations in alpha-actinin-2 cause hypertrophic cardiomyopathy: a genome-wide analysis. J Am Coll Cardiol. 2010;55(11):1127-35.

Clark KA, McElhinny AS, Beckerle MC, Gregorio CC. Striated muscle cytoarchitecture: an intricate web of form and function. Annu Rev Cell Dev Biol. 2002;18:637-706.

Clubb FJ Jr, Bishop SP. Formation of binucleated myocardial cells in the neonatal rat. An index for growth hypertrophy. Lab Invest. 1984;50(5):571-7.

Colson BA, Locher MR, Bekyarova T, Patel JR, Fitzsimons DP. Differential roles of regulatory light chain and myosin binding protein-C phosphorylations in the modulation of cardiac force development. J Physiol. 2010;588(6):981-93.

Crilley JG, Boehm EA, Blair E, et al. Hypertrophic cardiomyopathy due to sarcomeric gene mutations is characterized by impaired energy metabolism irrespective of the degree of hypertrophy. J Am Coll Cardiol 2003;41:1776-82.

Cummins P. Transitions in human atrial and ventricular myosin light-chain isoenzymes in response to cardiac-pressure-overload-induced hypertrophy. Biochem. J. 1982;205:195-204.

Dehaan RL, Eichna LW. Differentiation of the atrioventricular conducting system of the heart. Circulation. 1961;24:458-70.

De Jonge HW, Dekkers DH, Tilly BC, Lamers JM. Cyclic stretch and endothelin-1 mediated activation of chloride channels in cultured neonatal rat ventricular myocytes. Clin Sci (Lond). 2002;103(48):148S-151S.

Dorn GW, Force T. Protein kinase cascades in the regulation of cardiac hypertrophy. J Clin Invest. 2005;115(3):527–537.

Erickson JR, Joiner ML, Guan X, Kutschke W, Yang J et al. A dynamic pathway for calcium-independent activation of CaMKII by methionine oxidation. Cell. 2008;133(3):462-74.

Facundo HT, Brainard RE, Watson LJ, Ngoh GA, Hamid T, Prabhu SD, Jones SP. O-GlcNAc signaling is essential for NFAT-mediated transcriptional reprogramming during cardiomyocyte hypertrophy. Am J Physiol Heart Circ Physiol. 2012;302(10):H2122-30.

Fananapazir L, Epstein ND. Genotype-Phenotpe Correlations in Hypertrophic Cardiomyopathy Insights Provided by Comparisons of Kindreds With Distinct and Identical j3-Myosin Heavy Chain Gene Mutations. Circulation. 1994;89:22-32.

Geisterfer-Lowrance AA, Kass S, Tanigawa G, et al. A molecular basis for familial hypertrophic cardiomyopathy: a beta cardiac myosin heavy chain gene missense mutation. Cell 1990;62:999–1006.

Gurevich VV, Gurevich EV. The structural basis of arrestin-mediated regulation of G-protein-coupled receptors. Pharmacol Ther. 2006;110(3):465-502.

Hambleton M, York A, Sargent MA, Kaiser RA, Lorenz JN et al. Inducible and myocyte-specific inhibition of PKC enhances cardiac contractility and protects against infarction-induced heart failure. Am J Physiol Heart Circ Physiol 2007;293:3768–3771.

Harris SP, Lyons RG, Bezold KL. In the Thick of It: HCM-Causing Mutations in Myosin Binding Proteins of the Thick Filament. Circ Res. 2011;108:751-764.

Jarcho JA, McKenna W, Pare JA, et al. Mapping a gene for familial hypertrophic cardiomyopathy to chromosome 14q1. N Engl J Med 1989;321:1372– 8.

Jääskeläinen P, Heliö T, Aalto-Setälä K, Kaartinen M, Ilveskoski E, Hämäläinen L et al. Two founder mutations in the alpha-tropomyosin and the cardiac myosin-binding protein C genes are common causes of hypertrophic cardiomyopathy in the Finnish population. Annals of Medicine 2013;45:85–90.

Jääskeläinen P, Kuusisto J, Miettinen R, Kärkkäinen P, Kärkkäinen S et al. Mutations in the cardiac myosin-binding protein C gene are the predominant cause of familial

hypertrophic cardiomyopathy in eastern Finland. J Mol Med (Berl). 2002;80(7):412-22.

Jääskeläinen P, Soranta M, Miettinen R, Saarinen L, Pihlajamäki J et al. The cardiac beta-myosin heavy chain gene is not the predominant gene for hypertrophic cardiomyopathy in the Finnish population. J Am Coll Cardiol. 1998;32(6):1709-16.

Kamkin A, Kiseleva I, Isenberg G. Stretch-activated currents in ventricular myocytes: amplitude and arrhythmogenic effects increase with hypertrophy. Cardiovascular Research 2000;48:409–420.

Kamkin A, Kiseleva I, Isenberg G. A ctivation and inactivation of a non-selective cation conductance by local mechanical deformation of acutely isolated cardiac fibroblasts. Cardiovascular Research 2003;57:793–803.

Keung W, Boheler KR, Li RA. Developmental cues for the maturation of metabolic, electrophysiological and calcium handling properties of human pluripotent stem cell-derived cardiomyocytes. Stem Cell Res Ther. 2014;5(1):17.

Klues HG, Schiffers A, Maron BJ. Phenotypic Spectrum and Patterns of Left Ventricular Hypertrophy in Hypertrophic Cardiomyopathy: Morphologic Observations and Significance As Assessed by Two-Dimensional Echocardiography in 600 Patients. JACC 1995;26:1699-708.

Kubo T, Kitaoka H, Okawa M, Matsumura Y, Hitomi N, Yamasaki N, et al. Lifelong left ventricular remodeling of hypertrophic cardiomyopathy caused by a founder frameshift deletion mutation in the cardiac myosin-binding protein C gene among Japanese. J Am Coll Cardiol. 2005;46:1737 – 43.

Kujala K, Paavola J, Lahti A, Larsson K, Pekkanen-Mattila M, et al. Cell Model of Catecholaminergic Polymorphic Ventricular Tachycardia Reveals Early and Delayed Afterdepolarizations. PLoS ONE 2012;7(9):e44660.

Kulikovskaya I, McClellan G, Flavigny J, Carrier L, Winegrad S. Effect of MyBP-C binding to actin on contractility in heart muscle. J Gen Physiol. 2003;122(6):761-74.

Lammerding J, Kamm RD, Lee RT. Mechanotransduction in cardiac myocytes. Ann N Y Acad Sci. 2004;1015:53-70.

Lan F, Lee AS, Liang P et al. Abnormal Calcium Handling Properties Underlie Familial Hypertrophic Cardiomyopathy Pathology in Patient-Specific Induced Pluripotent Stem Cells. Cell Stem Cell 2013;12:101–113.

Landstrom AP, Ackerman MJ. Mutation type is not clinically useful in predicting prognosis in hypertrophic cardiomyopathy. Circulation. 2010;122(23):2441-9.

Lankford, EB, Epstein ND, Fananapazir L, Sweeney HL. Abnormal contractile properties of muscle fibers expressing b-myosin heavy chain gene mutations in patients with hypertrophic cardiomyopathy. J. Clin. Invest. 1995;95:1409-1414.

Liang P, Lan F, Lee AS, Gong T, Sanchez-Freire V, Wang Y et al. Drug screening using a library of human induced pluripotent stem cell-derived cardiomyocytes reveals disease-specific patterns of cardiotoxicity. Circulation. 2013;127(16):1677-91.

Liau B, Christoforou N, Leong KW, Bursac N. Pluripotent stem cell-derived cardiac tissue patch with advanced structure and function. Biomaterials. 2011;32(35):9180-7.

Lin D, Bobkova A, Homsher E, Tobacman LS. Altered cardiac troponin T in vitro function in the presence of a mutation implicated in familial hypertrophic cardiomyopathy. J Clin Invest. 1996;97:2842–2848.

Liu Z, Yue S, Chen X, Kubin T, Braun T. Regulation of cardiomyocyte polyploidy and multinucleation by CyclinG1. Circ Res. 2010;106(9):1498-506.

Lohse MJ, Engelhardt S, Eschenhagen T. What Is the Role of β-Adrenergic Signaling in Heart Failure? Circ Res. 2003;93:896-906.

Lundy SD, Zhu WZ, Regnier M, Laflamme MA. Structural and functional maturation of cardiomyocytes derived from human pluripotent stem cells. Stem Cells Dev. 2013;22(14):1991-2002.

Maron BJ, Gardin JM, Flack JM, Gidding SS, Kurosaki TT & Bild DE. Prevalence of hypertrophic cardiomyopathy in a general population of young adults: echocardiographic analysis of 4111 subjects in the CARDIA Study. Circulation 1995;92:785–89.

Maron BJ, Epstein SE, Roberts WC. Causes of sudden death in competitive athletes. J Am Coll Cardiol. 1986;7:204 –214.

Maron BJ, Maron MS. Hypertrophic cardiomyopathy. Lancet 2013;381:242–55.

Maron BJ, Roberts WC, McAllister HA, Rosing DR, Epstein SE. Sudden death in young athletes. Circulation. 1980;62:218 –229.

Maron MS, Maron BJ, Harrigan C, Buros J, Gibson CM et al. Hypertrophic Cardiomyopathy Phenotype Revisited After 50 Years With Cardiovascular Magnetic Resonance. JACC 2009;54(3):220-8.

Marston S, Copeland O, Jacques A, Livesey K, Tsang V, McKenna WJ, Jalilzadeh S, Carballo S, Redwood C, Watkins H. Evidence from human myectomy samples that MYBPC3 mutations cause hypertrophic cardiomyopathy through haploinsufficiency. Circ Res. 2009;105:219 –222.

Meurs KM, Mealey KL. Evaluation of the flanking nucleotide sequences of sarcomeric hypertrophic cardiomyopathy substitution mutations. Mutation Research 2008;642:86–89.

Metzger JM, Westfall MV. Covalent and noncovalent modification of thin filament action: the essential role of troponin in cardiac muscle regulation. Circ Res. 2004;94(2):146-58.

Mogensen J, Klausen IC, Pedersen AK, Egeblad H, Bross P et al. Alpha-cardiac actin is a novel disease gene in familial hypertrophic cardiomyopathy. J Clin Invest. 1999;103(10):39-43.

Mogensen J, Murphy RT, Kubo T, Bahl A, Moon JC et al. Frequency and clinical expression of cardiac troponin I mutations in 748 consecutive families with hypertrophic cardiomyopathy. J Am Coll Cardiol. 2004;44(12):2315-25.

Moolman-Smook JC, De Lange WJ, Bruwer EC, Brink PA, Corfield VA. The origins of hypertrophic cardiomyopathy-causing mutations in two South African subpopulations: a unique profile of both independent and founder events. Am J Hum Genet. 1999;65:1308 – 20.

Moorman AF, Christoffels VM. Cardiac chamber formation: development, genes, and evolution. Physiol Rev. 2003;83(4):1223-67.

Morimoto S, Yanaga F, Minakami R, Ohtsuki I. Ca2+-sensitizing effects of the mutations at Ile-79 and Arg-92 of troponin T in hypertrophic cardiomyopathy. Am J Physiol. 1998;275:C200–C207.

Morita H, Larson MG, Barr SC, Vasan RS, O'Donnell CJ et al. Single-gene mutations and increased left ventricular wall thickness in the community: the Framingham Heart Study. Circulation. 2006;113(23):2697-705.

Mummery CL, van Achterberg TA, van den Eijnden-van Raaij AJ, van Haaster L, Willemse A, de Laat SW, Piersma AH. Visceral-endoderm-like cell lines induce differentiation of murine P19 embryonal carcinoma cells. Differentiation. 1991;46(1):51-60.

Mummery C, Ward-van Oostwaard D, Doevendans P, Spijker R, van den BS, Hassink R, et al. Differentiation of human embryonic stem cells to cardiomyocytes: role of coculture with visceral endoderm-like cells. Circulation. 2003;107:2733–2740.

Mummery CL, Zhang J, Ng ES, Elliott DA, Elefanty AG, Kamp TJ. Differentiation of Human Embryonic Stem Cells and Induced Pluripotent Stem Cells to Cardiomyocytes: A Methods Overview. Circ Res. 2012;111:344-358.

Niimura H, Patton KK, McKenna WJ, Soults J, Maron BJ et al. Sarcomere Protein Gene Mutations in Hypertrophic Cardiomyopathy of the Elderly. Circulation. 2002;105:446-451.

Ohnuki M, Takahashi K, Yamanaka S. Generation and characterization of human induced pluripotent stem cells. Curr Protoc Stem Cell Biol. 2009;Chapter 4:Unit 4A.2.

Poetter K, Jiang H, Hassanzadeh S, Master SR, Chang A et al. Mutations in either the essential or regulatory light chains of myosin are associated with a rare myopathy in human heart and skeletal muscle. Nat Genet. 1996;13(1):63-9.

Ramirez MT, Zhao XL, Schulman H, Brown JH. The nuclear deltaB isoform of Ca2+/calmodulin-dependent protein kinase II regulates atrial natriuretic factor gene expression in ventricular myocytes. J Biol Chem. 1997;272(49):31203-8.

Rao C, Prodromakis T, Kolker L, Chaudhry UA, Trantidou T. The effect of microgrooved culture substrates on calcium cycling of cardiac myocytes derived from human induced pluripotent stem cells. Biomaterials. 2013;34(10):2399-411.

Rayment I, Holden HM, Sellers JR, Fananapazir L, Epstein ND. Structural interpretation of the mutations in the beta-cardiac myosin that have been implicated in familial hypertrophic cardiomyopathy. Proc Natl Acad Sci USA. 1995;92(9):3864-8.

Redwood C, Lohmann K, Bing W, Esposito GM, Elliott K, Abdulrazzak H et al. Investigation of a truncated cardiac troponin T that causes familial hypertrophic cardiomyopathy: $Ca^{(2+)}$ regulatory properties of reconstituted thin filaments depend on the ratio of mutant to wild-type protein. Circ Res. 2000;86:1146 –1152.

Richard P, Charron P, Carrier L, Ledeuil C, Cheav T et al. Hypertrophic Cardiomyopathy Distribution of Disease Genes, Spectrum of Mutations, and Implications for a Molecular Diagnosis Strategy. Circulation 2003;107:2227-2232.

Robertson C, Tran DD, George SC. Concise review: maturation phases of human pluripotent stem cell-derived cardiomyocytes. Stem Cells. 2013;31(5):829-37.

Robinson P, Griffiths PJ, Watkins H, Redwood CS. Dilated and hypertrophic cardiomyopathy mutations in troponin and alpha-tropomyosin have opposing effects on the calcium affinity of cardiac thin filaments. Circ Res 2007;101:1266-73.

Rose BA, Force T, Wang Y. Mitogen-activated protein kinase signaling in the heart: angels versus demons in a heart-breaking tale. Physiol Rev. 2010;90(4):1507-46.

Sadoshima J, Izumo S. The cellular and molecular response of cardiac myocytes to mechanical stress. Annu Rev Physiol. 1997;59:551-71.

Scholzen T, Gerdes J. The Ki-67 Protein: From the Known and the Unknown. J. Cell. Physiol. 2000;182:311–322.

Schiaffino S, Reggiani C. Molecular diversity of myofibrillar proteins: gene regulation and functional significance. Physiol Rev. 1996;76(2):371-423.

Seidman CE, Seidman JG. Identifying Sarcomere Gene Mutations in Hypertrophic Cardiomyopathy A Personal History. Circ Res. 2011;108:743-750.

Severs NJ. The cardiac muscle cell. Bioessays. 2000;22(2):188-99.

Soldner F, Laganière J, Cheng AW, Hockemeyer D, Gao Q. Generation of isogenic pluripotent stem cells differing exclusively at two early onset Parkinson point mutations. Cell. 2011;146(2):318–331.

Storchova Z, Pellman D. From polyploidy to aneuploidy, genome instability and cancer. Nat Rev Mol Cell Biol. 2004;5(1):45-54.

Sun N, Yazawa M, Liu J, Han L, Sanchez-Freire V, Abilez OJ et al. Patient-specific induced pluripotent stem cells as a model for familial dilated cardiomyopathy. Sci Transl Med. 2012;4(130):130-47.

Takahashi K, Tanabe K, Ohnuki M, Narita M, Ichisaka T et al. Induction of pluripotent stem cells from adult human fibroblasts by defined factors. Cell. 2007;131(5):861-72.

Takahashi K, Yamanaka S. Induction of pluripotent stem cells from mouse embryonic and adult fibroblast cultures by defined factors. Cell. 2006;126(4):663-76.

Tardiff JC. Thin Filament Mutations Developing an Integrative Approach to a Complex Disorder. Circ Res. 2011;108:765-782.

Van Berlo JH, Maillet M, Molkentin JD. Signaling effectors underlying pathologic growth and remodeling of the heart. 2013. J Clin Invest. 123(1):37-45.

Van Dijk SJ, Dooijes D, dos Remedios C, Michels M, Lamers JM, Winegrad S et al. Cardiac myosin-binding protein C mutations and hypertrophic cardiomyopathy: haploinsufficiency, deranged phosphorylation, and cardiomyocyte dysfunction. Circulation. 2009;119:1473–1483.

Wang Z, Zang C, Cui K, Schones DE, Barski A et al. Genome-wide mapping of HATs and HDACs reveals distinct functions in active and inactive genes. Cell. 2009;138(5):1019-31.

Warrick HM, Spudich JA. Myosin structure and function in cell motility. Annu Rev Cell Biol. 1987;3:379-421.

Watkins H, Ashrafian BM, Phil D, Redwood C. Inherited Cardiomyopathies. N Engl J Med 2011;364:1643-56.

Watkins H, McKenna WJ, Thierfelder L, Suk HJ, Anan R, O'Donoghue A et al. Mutations in the genes for cardiac troponin T and alpha-tropomyosin in hypertrophic cardiomyopathy. N Engl J Med. 1995;332:1058 –1064.

Watkins H, Rosenzweig A, Hwang DS, Levi T, McKenna W, Seidman CE, Seidman JG. Characteristics and prognostic implications of myosin missense mutations in familial hypertrophic cardiomyopathy. N Engl J Med. 1992;326:1108–1114.

Watkins H, Seidman CE, Seidman JG, Feng HS, Sweeney HL. Expression and functional assessment of a truncated cardiac troponin T that causes hypertrophic cardiomyopathy. Evidence for a dominant negative action. J. Clin. Invest. 1996;98:2456–2461.

Woo A, Rakowski H, Liew JC, Zhao M-S, Liew C-C. Mutations of the b myosin heavy chain gene in hypertrophic cardiomyopathy: critical functional sites determine prognosis. Heart 2003;89:1179–1185.

Yamasaki Y, Furuya Y, Araki K, Matsuura K, Kobayashi M, Ogata T. Ultra-high-resolution scanning electron microscopy of the sarcoplasmic reticulum of the rat atrial myocardial cells. Anat Rec. 1997;248(1):70-5.

Yang Q, Sanbe A, Osinska H, Hewett TE, Klevitsky R, Robbins J. In vivo modeling of myosin binding protein C familial hypertrophic cardiomyopathy. Circ Res. 1999;85:841– 847.

Zhang T, Kohlhaas M, Backs J, Mishra S, Phillips W et al. CaMKII delta isoforms differentially affect calcium handling but similarly regulate HDAC/MEF2 transcriptional responses. J Biol Chem. 2007;282(48):35078-87.